

Reversible reactions controlled by surface diffusion on a sphere

Denis S. Grebenkov^{1,*}

¹ *Laboratoire de Physique de la Matière Condensée (UMR 7643),
CNRS – Ecole Polytechnique, IP Paris, 91128 Palaiseau, France*
(Dated: September 30, 2019)

We study diffusion of particles on the surface of a sphere toward a partially reactive circular target with partly reversible binding kinetics. We solve the coupled diffusion-reaction equations and obtain the exact expressions for the time-dependent concentration of particles and the total diffusive flux. Explicit asymptotic formulas are derived in the small target limit. This study reveals the strong effects of reversible binding kinetics onto diffusion-mediated reactions that may be relevant for many biochemical reactions on cell membranes.

PACS numbers: 02.50.-r, 05.40.-a, 02.70.Rr, 05.10.Gg

Keywords: surface diffusion, reaction rate, cellular membrane, first passage time, reversible reaction

I. INTRODUCTION

Various vital processes occur on the cell membrane, examples ranging from cell signaling to ionic and molecular transfer [1]. In some cases, proteins diffuse on the cell membrane and search for specific receptors to trigger signal transduction via a cascade of biochemical reactions. For instance, G-protein-coupled receptors transmit their signals to the cell interior by interacting with G proteins and thus mediate the biological effects of many hormones and neurotransmitters [2]. A comprehensive theory of these crucial phenomena requires a better understanding of diffusive processes on two-dimensional surfaces and, in particular, on a spherical surface. In this direction, Bloomfield and Prager studied the impact of rotational diffusion on tail fiber attachment on bacteriophage T4 [3]. Assuming that the fiber tip diffuses freely over the surface of the sphere until it reaches a baseplate site, they computed the first two moments of the distribution of reaction times. Chao *et al.* investigated surface diffusion into a trap as a promising passive mechanism of localization of cell membrane components [4] (see also [5]). They derived the concentration of components by solving the time-dependent diffusion equation in the presence of a perfectly absorbing sink. Linderman and Lauffenburger analyzed trapping of diffusing receptors into tubules as a mechanism of intracellular receptor/ligand sorting [6]. Sano and Tachiya treated a more general case of imperfect sinks [7], for which they obtained the mean reaction time and discussed an exponential approximation for the survival probability. Berg considered the effect of weak binding of a diffusing particle to the nonspecific surface around a target on the sphere [8]. The resulting surface-mediated diffusion, in which three-dimensional diffusion in the bulk is coupled to two-dimensional diffusion on the surface, facilitates the target search. The optimality of such intermittent processes was further investigated [9–13]. Berg and Purcell estimated the reaction

rate controlled by bulk diffusion toward multiple small patches evenly distributed over the surface of a sphere [14]. This seminal paper and the associated homogenization concept were further extended by many authors [15–23]. Shoup *et al.* devised an efficient approximation to compute the reaction rate from the bulk to an active circular region on the surface of a sphere, even in the presence of rotational motion [24]. This approximation was further extended to compute the mean first-passage time (MFPT) from the bulk [25]. Singer *et al.* generalized the small-target asymptotic behavior of the MFPT to two-dimensional manifolds [26]. In turn, Coombs *et al.* derived the asymptotic behavior of the MFPT for a diffusing particle confined to the surface of a sphere, in the presence of many partially absorbing traps of small radii [27]. Prüstel and Tachiya considered the problem of reversible binding reactions on several two-dimensional domains, including the spherical case [28]. By employing convolution relations between the survival probabilities for reversible and irreversible reactions, they derived an exponential approximation for these probabilities.

In this paper, we further extend these former works by considering surface diffusion of particles on a sphere toward a partially reactive circular target with partly reversible binding kinetics (Sec. II). By generalizing the approach by Chao *et al.* [4], we provide in Sec. III the exact solution for the concentration of diffusing particles in both Laplace domain and time domain. In Sec. IV, we illustrate the properties of our solution, reveal the strong effects of reversible binding kinetics, and discuss implications for biochemical reactions on cell membranes. Explicit asymptotic formulas in the small target limit are also presented. Section V concludes the paper with the summary of results and perspectives for future research. Technical derivations are reported in Appendices.

II. MODEL

We consider the following model: a single particle A of radius ρ is fixed at the South pole of the sphere of radius R whereas point-like particles B diffuse on the surface of

*Electronic address: denis.grebenkov@polytechnique.edu

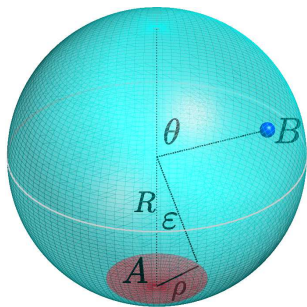
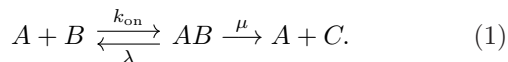


FIG. 1: Diffusion of a particle B (blue point) on the surface of a sphere toward a particle A (a target of angular size ε or, equivalently, of radius $\rho = R \sin \varepsilon$) fixed at the South pole (dark red region).

that sphere with the diffusion coefficient D (Fig. 1). In what follows, we call the particle A a target (or a sink, or a trap). This model can also describe the situation when the particle A diffuses with the coefficient D_A or/and when the particles B have a finite radius ρ_B . In this case, D is replaced by $D + D_A$ while ρ is replaced by $\rho + \rho_B$. However, the particles B are still assumed to be independent, without any mutual interaction (even without the excluded volume constraint). In practice, it means that the concentration of particles B should be rather dilute.

We study a common diffusion-influenced reaction



Once a particle B comes in contact with the target particle A , it can either bind with the target, or continue its diffusive motion on the surface. The probability of the binding event is determined by the reactivity κ (in units m/s) in a standard way [29–33]. The latter can also be related to the conventional association rate constant k_{on} (in units $\text{m}^2/\text{s}/\text{mol}$) as

$$k_{\text{on}} = \kappa N_A (2\pi\rho), \quad (2)$$

where $N_A \simeq 6 \cdot 10^{23}$ 1/mol is the Avogadro number, and $2\pi\rho$ is the target perimeter [34, 35] (another notation, $k_d = k_{\text{on}}/N_A = 2\pi\rho\kappa$, was employed in [28, 36]). A finite reactivity κ mimics conformational or energy activation barrier that the particles A and B have to overcome to form a metastable complex AB . Two rates λ and μ allow us to distinguish three scenarios of irreversible ($\lambda = 0$), reversible ($\lambda > 0$, $\mu = 0$), and partly reversible ($\lambda > 0$, $\mu > 0$) binding. When the dissociation (or desorption) rate λ is zero, the particle B never resumes its diffusion, being either chemically transformed into another particle C with the rate μ , or staying bound forever to the target (if $\mu = 0$). In the former case, the target A plays the role of a catalyst for the transformation of B into C . When $\lambda > 0$ and $\mu = 0$, the formation of the complex AB is fully reversible, i.e., the particle B remains

bound for a random exponentially distributed time, determined by the dissociation rate λ , and then resumes its surface diffusion until the next binding. This mechanism accounts for reversible reactions [36–39]. In turn, the last case $\lambda > 0$ and $\mu > 0$ describes partly reversible scenario when the metastable complex AB can dissociate either into $A + B$ with the rate λ (in which case B resumes its diffusion until the next binding), or into $A + C$ with the rate μ . Note that the rate λ was also denoted as k_{off} or k_a .

In spherical angular coordinates (θ, φ) , the diffusion domain on the surface of the sphere is $\Omega = \{(\theta, \varphi) : 0 \leq \theta < \pi - \varepsilon, 0 \leq \varphi < 2\pi\}$, whereas the target surface is $\partial\Omega = \{(\theta, \varphi) : \theta = \pi - \varepsilon, 0 \leq \varphi < 2\pi\}$, where ε is the angular size of the target: $\rho = R \sin \varepsilon$. We introduce the surface concentration of particles B in a point (θ, φ) , $c(\theta, \varphi, t)$ (in mol/m^2) that obeys the diffusion equation

$$\partial_t c = D \Delta c \quad \text{in } \Omega, \quad (3)$$

where Δ is the Laplace-Beltrami operator on the sphere:

$$\Delta = \frac{1}{R^2} \left(\frac{1}{\sin \theta} \partial_\theta \sin \theta \partial_\theta + \frac{1}{\sin^2 \theta} \partial_\varphi^2 \right). \quad (4)$$

Even though a Dirac point-like source would yield a more general description, we restrict the analysis to the uniform initial concentration of particles B :

$$c(\theta, \varphi, t = 0) = C_0. \quad (5)$$

This assumption, which is rather common for applications, simplifies technical computations. In fact, the axial symmetry of the domain and of the initial condition ensures that the solution $c(\theta, \varphi, t)$ does not depend on the azimuthal angle φ that we drop in the following. It is worth noting that the developed method can be extended to a general setting without axial symmetry.

The diffusion equation (3) is completed by the Robin boundary condition on the target boundary $\partial\Omega$

$$-D(\partial_n c)|_{\partial\Omega} = \kappa c|_{\partial\Omega} - \lambda \frac{n_T}{2\pi\rho}, \quad (6)$$

where $\partial_n = (1/R)\partial_\theta$ is the normal derivative directed toward the target, and $n_T(t)$ (in mol) is the amount of particles B bound to the target at time t . Here, $n_T/(2\pi\rho)$ can be understood as the density of bound particles along the target boundary of length $2\pi\rho$. In chemical physics, the relation (6) is called “back-reaction”, “generalized radiation”, or “generalized Collins-Kimball” boundary condition [28, 38–40]. It states that the net diffusive flux density of particles B toward the target (the left-hand side) is equal to the reactive flux density, $\kappa c|_{\partial\Omega}$, minus the flux density related to the dissociation of the metastable complex AB (the last term). The reactivity κ characterizes the difficulty for a particle B to overcome an energy activation barrier for binding to the target [41–43] (see also a recent overview in [44, 45]). The limit $\kappa = \infty$ describes an immediate reaction upon the first encounter

(no activation barrier), whereas $\kappa = 0$ corresponds to no reaction (infinite activation barrier) on reflecting boundary. The concentration is also required to be regular (not diverging) at the North pole that will serve as the second boundary condition at $\theta = 0$, see below.

In turn, the amount of particles B bound to the target, $n_T(t)$, obeys the first-order differential equation:

$$\partial_t n_T = J(t) - \mu n_T, \quad (7)$$

with the initial condition $n_T(t=0) = 0$, where

$$J(t) = \int_{\partial\Omega} dl (-D(\partial_n c)|_{\partial\Omega}) = -2\pi\rho D(\partial_n c)|_{\partial\Omega} \quad (8)$$

is the total diffusive flux onto the target, and the second term accounts for irreversible transformation of the metastable complex AB into A and C . Once $J(t)$ is found, one gets immediately

$$n_T(t) = \int_0^t dt' e^{-\mu(t-t')} J(t'). \quad (9)$$

In the case $\mu > 0$, the amount $n_C(t)$ of produced particles C obeys an ordinary differential equation,

$$\partial_t n_C(t) = \mu n_T(t), \quad (10)$$

with the initial condition $n_C(0) = 0$. Once $n_T(t)$ is found, $n_C(t)$ follows immediately by integration.

III. SOLUTION

In this section, we solve the coupled partial differential equations introduced in Sec. II. As it is common for diffusion problems, we first obtain the solution in Laplace domain (for Laplace-transformed quantities) and then proceed to the solution in time domain via Laplace transform inversion.

A. Solution in Laplace domain

Setting

$$x = \cos \theta, \quad (11)$$

the Laplace-Beltrami operator can be written as

$$\Delta = \mathcal{L}/R^2, \quad \mathcal{L} = \partial_x(1-x^2)\partial_x. \quad (12)$$

In order to get rid of the derivative with respect to time t , the Laplace transform is performed,

$$\tilde{c}(x, s) = \int_0^\infty dt e^{-ts} c(x, t), \quad (13a)$$

$$\tilde{n}_T(s) = \int_0^\infty dt e^{-ts} n_T(t) \quad (13b)$$

(throughout the paper, tilde denotes Laplace-transformed quantities). The new functions $\tilde{c}(x, s)$ and $\tilde{n}_T(s)$ satisfy

$$s\tilde{c}(x, s) - \frac{D}{R^2} \mathcal{L}\tilde{c}(x, s) = C_0, \quad (14a)$$

$$(s + \lambda + \mu) \frac{\tilde{n}_T(s)}{2\pi\rho} = \kappa \tilde{c}(a, s), \quad (14b)$$

$$\frac{D}{R} \sqrt{1-a^2} (\partial_x \tilde{c}(x, s))_{x=a} = \kappa \tilde{c}(a, s) - \frac{\lambda \tilde{n}_T(s)}{2\pi\rho}, \quad (14c)$$

where we used $\partial_n = -(1/R) \sin \theta \partial_x$, the initial condition $n_T(t=0) = 0$, and

$$a = \cos(\pi - \varepsilon) = -\cos \varepsilon = -\sqrt{1 - (\rho/R)^2} \quad (15)$$

is the location of the target surface $\partial\Omega$. As Eq. (14b) relates $\tilde{n}_T(s)$ and $\tilde{c}(a, s)$, one can rewrite Eq. (14c) as Robin boundary condition

$$(\partial_x \tilde{c}(x, s))_{x=a} = q_s \tilde{c}(a, s), \quad (16)$$

with

$$q_s = q \frac{s + \mu}{s + \lambda + \mu}, \quad (17)$$

where

$$q = \frac{\bar{\kappa}}{\sqrt{1-a^2}} \geq 0, \quad \bar{\kappa} = \frac{\kappa R}{D} \quad (18)$$

(throughout the paper, bar denotes dimensionless quantities rescaled by R and D). In other words, the above coupled differential equations for c and n_T are decoupled in Laplace domain and reduced to a single differential equation

$$(R^2 s/D - \mathcal{L})\tilde{c} = \frac{R^2 C_0}{D} \quad (a < x < 1), \quad (19)$$

subject to the Robin boundary condition (16) at $x = a$ (the target), and the regularity condition at $x = 1$ (the North pole). This implies that the reversible kinetics can be described in Laplace domain as irreversible one, with a “frequency”-dependent reactivity

$$\kappa(s) = \kappa \frac{s + \mu}{s + \lambda + \mu}. \quad (20)$$

In time domain, this would result in a convolution-type Robin boundary condition with an “effective” time-dependent reactivity. We note that Eqs. (16, 17) present an extension of the well-known back-reaction boundary condition in Laplace domain (see, e.g., [28, 36]) by accounting for the rate μ .

The solution of the above equation can be obtained in terms of the Legendre functions of the first kind, $P_\nu(x)$, that satisfy the Legendre equation on $a < x < 1$,

$$\underbrace{\partial_x(1-x^2)\partial_x}_{\mathcal{L}} P_\nu(x) + \nu(\nu+1)P_\nu(x) = 0, \quad (21)$$

and are regular at $x = 1$ (see Appendix A for some properties of these functions). The Robin boundary condition at $x = a$ reads

$$P'_\nu(a) = q_s P_\nu(a), \quad (22)$$

where the prime denotes the derivative with respect to x : $P'_\nu(a) = (\partial_x P_\nu(x))_{x=a}$. As a and q_s are fixed, this is an equation on the degree ν that has infinitely many real-valued solutions, denoted as ν_n^s , with $n = 0, 1, 2, \dots$ (see Appendix B 1):

$$0 \leq \nu_0^s \leq \nu_1^s \leq \dots \nearrow +\infty \quad (23)$$

(negative solutions are not considered because of the symmetry: $P_\nu(x) = P_{-\nu-1}(x)$). The eigenvalues of the operator $-\mathcal{L}$ are then $\nu_n^s(\nu_n^s + 1)$. We emphasize that ν_n^s and thus the eigenfunctions $P_{\nu_n^s}(x)$ depend on s through the parameter q_s in the Robin boundary condition (22).

As the operator \mathcal{L} is self-adjoint, its eigenfunctions $P_{\nu_n^s}(x)$ form a complete basis in the space of square-integrable functions on $(a, 1)$. As a consequence, one can search for a solution of Eq. (19) in the form

$$\tilde{c}(x, s) = \sum_{n=0}^{\infty} a_n(s) b_n P_{\nu_n^s}(x), \quad (24)$$

where the constants b_n ensure the L_2 -normalization of $P_{\nu_n^s}(x)$,

$$b_n = \left(\int_a^1 dx [P_{\nu_n^s}(x)]^2 \right)^{-1/2} \quad (25)$$

(see the identity (A9) for computing these constants). The unknown coefficients $a_n(s)$ can be found by substituting the ansatz (24) into Eq. (19), multiplying by $P_{\nu_n^s}(x)$, integrating from a to 1, and using the orthogonality of $P_{\nu_n^s}(x)$ (see Appendix B 1):

$$a_n(s) = \frac{C_0 b_n}{s + D\nu_n^s(\nu_n^s + 1)/R^2} \int_a^1 dx P_{\nu_n^s}(x). \quad (26)$$

The integral of the Legendre function can be easily calculated via Eq. (A4), yielding

$$\tilde{c}(x, s) = C_0(1-a^2) \sum_{n=0}^{\infty} \frac{b_n^2 P_{\nu_n^s}(x) P'_{\nu_n^s}(a)}{\nu_n^s(\nu_n^s + 1)(s + D\nu_n^s(\nu_n^s + 1)/R^2)}. \quad (27)$$

While we used here the uniform initial condition for $c(x, t)$, one can substitute it by any given (axially symmetric) initial condition, including the Dirac distribution $\delta(x - x_0)$, in which case the integral of $P_{\nu_n^s}(x)$ in Eq. (26) would simply yield $P_{\nu_n^s}(x_0)$.

From Eqs. (8, 27), one deduces the Laplace transform of the total diffusive flux onto the target:

$$\tilde{J}(s) = 2\pi C_0 D(1-a^2)^2 \sum_{n=0}^{\infty} \frac{b_n^2 [P'_{\nu_n^s}(a)]^2}{\nu_n^s(\nu_n^s + 1)(s + \frac{D}{R^2} \nu_n^s(\nu_n^s + 1))}. \quad (28)$$

Eqs. (27, 28) constitute the exact solution of the problem in Laplace domain.

B. Solution in time domain

The Laplace transform inversion can be performed with the aid of the residue theorem that requires finding the poles of Eq. (27) in the complex plane of s . We recall that ν_n^s and thus b_n and $P_{\nu_n^s}(x)$ depend on s through the parameter q_s in the Robin boundary condition (22). Since we deal with a diffusion problem, the poles should lie exclusively on the negative real axis. We expect that $P_{\nu_n^s}(x)$ as a function of s does not have poles (see a short comment in Appendix B 1, even though a rigorous proof of this claim is beyond the scope of this paper) so that the poles come from the zeros of the denominator in Eq. (27). In the particular case $\lambda > 0$ and $\mu = 0$, the solution reaches a nontrivial steady-state limit with $\nu = 0$ which is determined by the pole $s = 0$ that we will treat separately (in other cases, this pole does not appear). The other poles are strictly negative and determined as the zeros of the functions

$$f_n(s) \equiv s + \frac{D}{R^2} \nu_n^s(\nu_n^s + 1) = 0. \quad (29)$$

Since ν_n^s as solutions of Eq. (22) depend on s , one has to search for a pair (s, ν) as a solution of the system of two nonlinear equations (22, 29). Expressing s from Eq. (29) in terms of ν_n^s , one reduces this system to a single equation

$$(\bar{\lambda} + \bar{\mu} - \nu(\nu + 1))P'_\nu(a) = q(\bar{\mu} - \nu(\nu + 1))P_\nu(a), \quad (30)$$

with dimensionless rates

$$\bar{\lambda} = \lambda R^2/D, \quad \bar{\mu} = \mu R^2/D, \quad (31)$$

and q is given by Eq. (18). In Appendix B 2, we prove that all the solutions of this equation are real; moreover, negative solutions are ignored due to the symmetry $P_\nu(x) = P_{-\nu-1}(x)$. We denote the positive solutions as

$$0 \leq \nu_0 \leq \nu_1 \leq \dots \nearrow +\infty \quad (32)$$

(without the superscript s) to distinguish them from ν_n^s . The poles are simply

$$s_n = -D\nu_n(\nu_n + 1)/R^2. \quad (33)$$

As ν_n obeys the boundary condition (22) for such s that satisfies Eq. (29), one can formally write $\nu_n = \nu_n^{s_n}$.

Quite unusually, the numerical computation in time domain turns out to be simpler than that in the Laplace domain, because the set of solutions of Eq. (30) has to be computed only once, whereas solutions of Eq. (22) had to be found for each value of s .

If all poles s_n are simple, then the inverse Laplace transform of the concentration reads

$$c(x, t) = C_0 \sum_{n=0}^{\infty} c_n e^{-Dt\nu_n(\nu_n+1)/R^2} P_{\nu_n}(x), \quad (34)$$

$$c_n = (1 - a^2) \frac{b_n^2 P'_{\nu_n}(a)}{\nu_n(\nu_n + 1)(\partial_s f_n)(s_n)}, \quad (35)$$

and that of the total flux is

$$J(t) = C_0 D \sum_{n=0}^{\infty} J_n e^{-Dt\nu_n(\nu_n+1)/R^2}, \quad (36)$$

$$J_n = 2\pi(1 - a^2)^2 \frac{b_n^2 [P'_{\nu_n}(a)]^2}{\nu_n(\nu_n + 1)(\partial_s f_n)(s_n)}. \quad (37)$$

In Appendix B3, we show how the contribution $(\partial_s f_n)(s_n)$ to each residue can be computed in practice, whereas Appendix C presents an example of such computation.

Finally, we also get from Eqs. (9, 10, 36):

$$n_T(t) = C_0 D \sum_{n=0}^{\infty} J_n \frac{e^{-\mu t} - e^{-Dt\nu_n(\nu_n+1)/R^2}}{D\nu_n(\nu_n + 1)/R^2 - \mu} \quad (38)$$

(note that if μ coincides with $D\nu_n(\nu_n + 1)/R^2$ for some n , the corresponding term would be $J_n t e^{-\mu t}$; similarly, a specific term appears in the case when $\mu = 0$ and $\nu_0 = 0$) and

$$n_C(t) = \mu C_0 D \sum_{n=0}^{\infty} \frac{J_n}{D\nu_n(\nu_n + 1)/R^2 - \mu} \times \left(\frac{1 - e^{-\mu t}}{\mu} - \frac{1 - e^{-Dt\nu_n(\nu_n+1)/R^2}}{D\nu_n(\nu_n + 1)/R^2} \right) \quad (39)$$

(again, a specific term appears if μ coincides with $D\nu_n(\nu_n + 1)/R^2$ for some n). With these expressions, we completed obtaining the exact solution of our model of diffusion-influenced reactions on the sphere.

IV. DISCUSSION

In this section, we discuss the main features of the derived solutions.

A. Conservation of particles

When $\mu = 0$, the total number of particles B is preserved. In fact, integrating Eq. (3) over the domain Ω , we get an equation for the total number of particles diffusing on the sphere:

$$\partial_t N(t) = D \int_{\Omega} ds \Delta c = \int_{\partial\Omega} dl (D\partial_n c)|_{\partial\Omega} = -\partial_t n_T(t), \quad (40)$$

with the last equality coming from Eq. (7). The total number of particles, $N(t) + n_T(t)$, is thus preserved:

$$N(t) + n_T(t) = N(0) + n_T(0) = 2\pi(1 - a)R^2 C_0, \quad (41)$$

where we used the initial conditions $c(x, t = 0) = C_0$ and $n_T(t = 0) = 0$.

In the steady-state limit (as $t \rightarrow \infty$), the populations of particles on the surface and on the target are equilibrated. As the steady-state flux is zero, Eq. (6) implies

$$c_{\infty} = c(x, t = \infty) = \frac{\lambda}{2\pi\rho\kappa} n_T(t = \infty), \quad (42)$$

from which Eq. (41) yields

$$c_{\infty} = C_0 \left(1 + \frac{\kappa}{\lambda R} \sqrt{\frac{1+a}{1-a}} \right)^{-1}. \quad (43)$$

This expression results from the detailed balance between free and bound particles B , which is controlled by the reactivity κ and the dissociation rate λ .

B. Survival probabilities

While the above discussion dealt with the concentration $c(x, t)$ of particles on the sphere, it is instructive to provide its probabilistic interpretation. Given that the initial concentration was set to be a constant C_0 , the dimensionless ratio $c(x, t)/C_0$ can be interpreted as the probability of finding a particle B , that started from a point $x = \cos\theta$ at time 0, in the free state (not bound to the target) at a later time t . For irreversible reactions, it is called the survival probability [46] because irreversible binding to the target can be understood as “killing” of a free particle B . The same term was adopted by Agmon *et al.* for reversible reactions in [28, 36, 38], in which $c(x, t)/C_0$ was denoted as $S_{\text{rev}}(t|x)$.

Moreover, Agmon *et al.* also considered the probability $S_{\text{rev}}(t|*)$ for a particle, that was initially in the bound state, to be unbound in a later time t . This probability was expressed in terms of $S_{\text{rev}}(t|a)$ (see [36], Eq. (3.15)). Comparing that relation with Eq. (14b) at $\mu = 0$, one can identify

$$S_{\text{rev}}(t|*) = \frac{\lambda}{2\pi\rho\kappa C_0} n_T(t). \quad (44)$$

The explicit solution (38) yields thus

$$S_{\text{rev}}(t|*) = \frac{\lambda R^2}{2\pi\rho\kappa} \sum_{n=0}^{\infty} J_n \frac{1 - e^{-Dt\nu_n(\nu_n+1)/R^2}}{\nu_n(\nu_n + 1)}. \quad (45)$$

In the long-time limit, this probability approaches a steady-state limit, which can be either obtained from the above spectral decomposition, or from Eqs. (42, 43, 44):

$$S_{\text{rev}}(t = \infty|*) = \left(1 + \frac{\kappa}{\lambda R} \sqrt{\frac{1+a}{1-a}} \right)^{-1}. \quad (46)$$

This probability is smaller than 1, in contrast to the case of diffusion in unbounded domains outside a disk or a sphere, studied in [36, 47, 48], for which $S_{\text{rev}}(t = \infty|*) = 1$.

We also note that Eq. (7) with $\mu = 0$ implies that the time derivative of $S_{\text{rev}}(t|*)$ gives back the total flux $J(t)$, so that one recovers the relation (3.17) from [36] for the time-dependent rate coefficient:

$$k_{\text{rev}}(t) = \frac{J(t)}{C_0} = \frac{\partial_t n_T(t)}{C_0} = \frac{2\pi\rho\kappa}{\lambda} \partial_t S_{\text{rev}}(t|*). \quad (47)$$

In the following, we focus on the concentration $c(x, t)$ and the total flux $J(t)$, bearing in mind that other important quantities can be directly accessed.

C. Limiting cases

Our solution generalizes previous works on diffusion-influenced reactions on the spherical surface. We discuss several limiting cases which yield simpler formulas.

Irreversible reactions

For irreversible reactions ($\lambda = 0$), a particle B that is bound to the target, is never released. As a consequence, the boundary condition (6) for the concentration c is decoupled from n_T , so that one can solve first the boundary value problem for c with Robin boundary condition, evaluate the diffusive flux $J(t)$, and then determine n_T from Eq. (7). In fact, Eq. (17) is reduced to $q_s = q$, so that Robin boundary condition (22) reads

$$P'_\nu(a) = qP_\nu(a). \quad (48)$$

Its solutions ν_n^s do not depend on s and actually coincide with the solutions of ν_n of Eq. (30). As a consequence,

$$(\partial_s f_n)(s_n) = 1, \quad (49)$$

and Eqs. (35, 37) are simplified. In the following, we refer to the corresponding concentration and total flux as $c_0(x, t)$ and $J_0(t)$, where subscript 0 highlights that this solution corresponds to $\lambda = 0$. This is a generalization of the solution presented in Ref. [4] to the case of a partially absorbing sink.

Whenever $a < 1$ and $\kappa > 0$ (i.e., a nontrivial partially reactive target is present), it is easy to check that the first solution ν_0 of Eq. (48) is strictly positive (in fact, if ν_0 was equal to 0, then $P_{\nu_0}(x) = 1$ and thus Eq. (48) cannot be satisfied). As a consequence, the concentration of particles $c_0(x, t)$ and the flux $J_0(t)$ vanish as $t \rightarrow \infty$.

Perfect sink

For a perfect sink ($\kappa = \infty$), the Robin boundary condition (22) is reduced to the Dirichlet condition (also

known as totally absorbing or Smoluchowski boundary condition) $c|_{\partial\Omega} = 0$ that reads as

$$P_\nu(a) = 0, \quad (50)$$

which does not depend on s . As a consequence, Eq. (49) holds again, and the concentration $c(x, t)$ and the diffusive flux $J(t)$ are still determined by Eqs. (34, 36), in which ν_n are the solutions of Eq. (50). This is precisely the solution presented in Ref. [4]. Note that when the sink is perfect, it does not matter whether the reaction is reversible or not: any released particle will be immediately re-adsorbed by the target.

Steady-state regime

For reversible reactions with $\mu = 0$, a steady-state solution is established at long times so that there should exist an eigenmode with $\nu = 0$. First, using the properties of Legendre functions, we rewrite (22) as

$$[a(\nu + 1) - (1 - a^2)q_s]P_\nu(a) = (\nu + 1)P_{\nu+1}(a). \quad (51)$$

Searching for ν_0 in the form ηs^α (with some constant η and degree α) and substituting it into Eq. (51), we get with the aid of Eqs. (A13)

$$\nu_0 \simeq \eta s + O(s^2), \quad \text{with } \eta = \frac{\kappa R}{D\lambda} \sqrt{\frac{1+a}{1-a}}, \quad (52)$$

from which $P_{\nu_0}(x) \simeq 1 + O(s)$, $P'_{\nu_0}(a) = q_s + O(s^2)$, $b_n^2 \simeq (1 - a)^{-1}$, and thus the leading term of Eq. (27) behaves asymptotically as

$$\tilde{c}(x, s) \simeq \frac{C_0}{(1 + D\eta/R^2)s} \quad (s \rightarrow 0). \quad (53)$$

Inverting the Laplace transform, we retrieve a uniform steady-state concentration in Eq. (43).

D. Numerical implementation

The concentration $c(x, t)$ and the total flux $J(t)$ are given via exact spectral decompositions (34, 36). Since the solutions ν_n grow up to infinity as $n \rightarrow \infty$, both decompositions converge exponentially fast for any fixed $t > 0$. As time t stands in front of $\nu_n(\nu_n + 1)$ in the exponential function, larger Dt/R^2 yields faster convergence. In turn, the effect of other parameters on the convergence speed is more subtle and requires a systematic analysis that is beyond the scope of this paper.

In practice, the spectral decompositions have to be truncated up to some order n_{max} , which can be selected according to the minimal time at which $c(x, t)$ and $J(t)$ need to be calculated. The properties of the Legendre function $P_\nu(x)$ summarized in Appendix A were thoroughly used for efficient numerical computations. In particular, $P_\nu(x)$ and its derivatives with respect to x and

ν were accurately and rapidly computed via Eqs. (A14, A6, A15). Using bisection or Newton's method, one computes numerically the needed number of the solutions ν_n of Eq. (30). These solutions then determine the poles s_n , the normalization constants b_n and the contribution $(\partial_s f_n)(s_n)$ to each residue (see Appendix B3 for details), from which the coefficients c_n and J_n are computed via Eqs. (35, 37). Note that if some poles are not simple, their contribution to the spectral decompositions (34, 36) should be modified according the residue theorem; in practice, the poles were simple in all considered examples. In Appendix C, we illustrate this numerical scheme by computing the total flux.

E. Comparison with Tachiya's approach

In his seminal work [37], Tachiya proposed an elegant approach to relate the solutions for reversible and irreversible reactions (see also [28, 36]). His straightforward probabilistic arguments couple $c(x, t)$ for reversible reactions (with $\lambda > 0$) to $c_0(x, t)$ for irreversible reactions (with $\lambda = 0$) via convolution relations that can be easily solved in the Laplace domain. In our notations, one gets

$$\tilde{c}(x, s) = \frac{1}{s} + \frac{\tilde{c}_0(x, s) - 1/s}{1 + \lambda \tilde{c}_0(a, s) s / (s + \mu)}, \quad (54)$$

where we also included the rate μ . One can easily check that the function $\tilde{c}(x, s)$ satisfies Eqs. (14a, 19) with q_s from Eq. (17), given that $\tilde{c}_0(x, s)$ satisfies Eqs. (14a, 19) with q instead of q_s . This is a significant simplification because Eq. (27) for $\tilde{c}_0(x, s)$ involves ν_n^s that do not depend on s and thus have to be computed only once. However, the simple and instructive relation (54) in the Laplace domain is not much helpful for the Laplace inversion. In contrast, our approach allows one to get the exact solutions in time domain so that two approaches are complementary to each other.

We also note that our description with $\mu = 0$ is equivalent to that given by Prüstel and Tachiya [28]. In fact, the boundary condition (6) can be re-written in the form of Eq. (16) from Ref. [28]:

$$2\pi\rho\frac{D}{R}\sin\varepsilon\partial_x c|_{\partial\Omega} = k_a c|_{\partial\Omega} - k_d \left(1 - 2\pi R^2 \int_a^1 dx' c(x', t)\right), \quad (55)$$

with $k_a = 2\pi\rho\kappa$, $k_d = \lambda$, and

$$n_T(t) = 1 - 2\pi R^2 \int_a^1 dx' c(x', t). \quad (56)$$

The time derivative of the last equation yields, after simplifications, Eq. (7).

Instead of solving exactly the problem for irreversible kinetics, Prüstel and Tachiya used an exponential ap-

proximation for the survival probability,

$$S_0(x, t) = \frac{c_0(x, t)}{C_0} \approx \exp(-t/\tau(x)), \quad (57)$$

where $\tau(x)$ is the mean first passage time in the case of irreversible reaction (with $\lambda = 0$):

$$\tau(x) = \int_0^\infty dt S_0(x, t), \quad (58)$$

which was found in [7] (see also Appendix D):

$$\tau(x) = \frac{R^2}{D} \ln\left(\frac{1+x}{1+a}\right) + \frac{R}{\kappa} \sqrt{\frac{1-a}{1+a}}. \quad (59)$$

With this approximation, the Laplace inversion of Eq. (54) yielded an approximate formula for the concentration $c(x, t)$ which reads in our notations as

$$\frac{c(x, t)}{C_0} \simeq \frac{\lambda}{\lambda + \frac{1}{\tau(a)}} + e^{-t/\tau(x)} \frac{\frac{1}{\tau(x)} - \frac{1}{\tau(a)}}{\frac{1}{\tau(x)} - \frac{1}{\tau(a)} - \lambda} - e^{-t(\lambda + 1/\tau(a))} \left[\frac{\lambda}{\lambda + \frac{1}{\tau(a)}} + \frac{\lambda}{\frac{1}{\tau(x)} - \frac{1}{\tau(a)} - \lambda} \right]. \quad (60)$$

Since the validity of this approximation was not tested in [28], we undertake this study here. Figure 2 illustrates the quality of the exponential approximation (57) for irreversible reactions. When the particle B starts far from a small perfectly absorbing target ($x = 0$, $\kappa = \infty$, Fig. 2a), the diffusive search takes long time that is enough for a particle to “forget” about its starting point. In this setting, Eq. (57) accurately approximates the survival probability. In contrast, when the starting point is close to the target ($x = -\cos(2\varepsilon) \approx -0.866$), there are high changes of finding it in a short time, and the exponential approximation (57) fails. It is also worth noting that the exponential asymptotic decay of the survival probability $S_0(x, t)$ is determined by the smallest eigenvalue of the diffusion operator, which is independent of the starting point. In this light, the approximation (57) can only be valid when $\tau(x)$ is close to $T = R^2/(D\nu_0(\nu_0 + 1))$ and thus independent of x , requiring the starting point to be far from the target and the target to be small. The situation is different for weakly reactive target with $\kappa R/D = 1$ (Fig. 2b). Even when the starting point is close to the target, multiple failed attempts of binding to the target allow for the particle to explore the whole domain until the successful binding. In other words, the second term in Eq. (59) is dominant, whereas the dependence on the starting point x is irrelevant. In summary, for a fixed x , the approximation (60) is getting more accurate when the target size and/or reactivity decrease. In particular, this approximation can be employed to re-derive the asymptotic behavior of the total flux in the small-target limit, as an alternative to the rigorous analysis presented in Sec. IV F. At the same time, the dependence on the

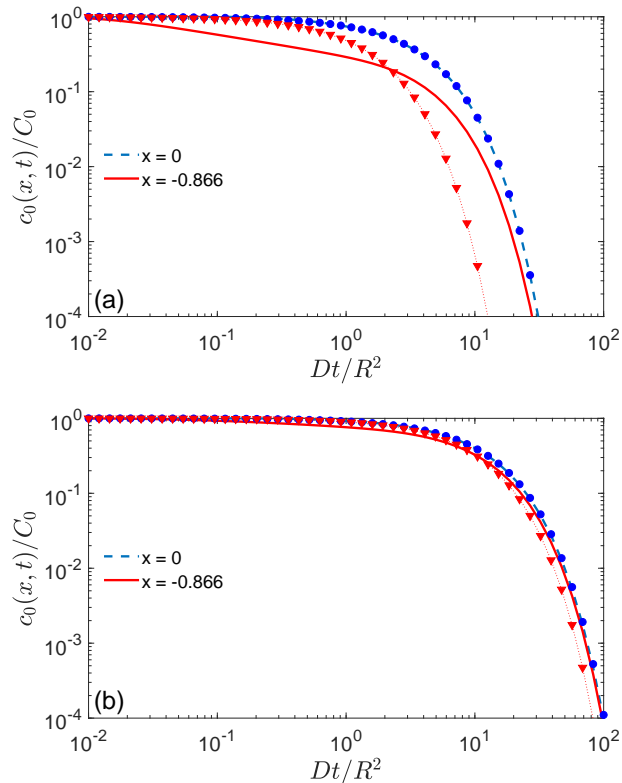


FIG. 2: The normalized concentration $c_0(x, t)/C_0$ for irreversible reactions ($\lambda = 0$) as a function of rescaled time Dt/R^2 , for a target of angular size $\varepsilon = \pi/12$, and two starting points: $x = 0$ (the equator) and $x = \cos(\pi - 2\varepsilon) \approx -0.886$ (close to the target). Lines show the exact solution (34), truncated at $n_{\max} = 50$, while symbols present the exponential approximation (57). (a) Perfectly reactive target ($\kappa R/D = \infty$); (b) partially reactive target ($\kappa R/D = 1$).

starting point is not captured, and the approximation fails when the starting point is close to a highly reactive target, irrespectively of its size. In this light, an even simpler approximation $S_0(x, t) \approx \exp(-t/\tau(0))$ would be more natural.

Figure 3 shows the normalized concentration $c(x, t)/C_0$ for reversible reactions (with $\lambda > 0$ and $\mu = 0$) as a function of rescaled time Dt/R^2 for the same target and the same starting points. As a perfectly reactive target would yield irreversible reactions, we do not consider the case $\kappa = \infty$ but compare two cases with high reactivity $\kappa R/D = 10$ and weak reactivity $\kappa R/D = 1$. To keep the same steady-state concentration c_∞ , we set $\lambda R^2/D = 1$ and $\lambda R^2/D = 0.1$, respectively. As discussed previously for irreversible reactions, the approximate solution (60) fails when the starting point is close to the target, even for weakly reactive target. In turn, the approximation is getting more accurate when the starting point is far from the target and the reactivity is low.

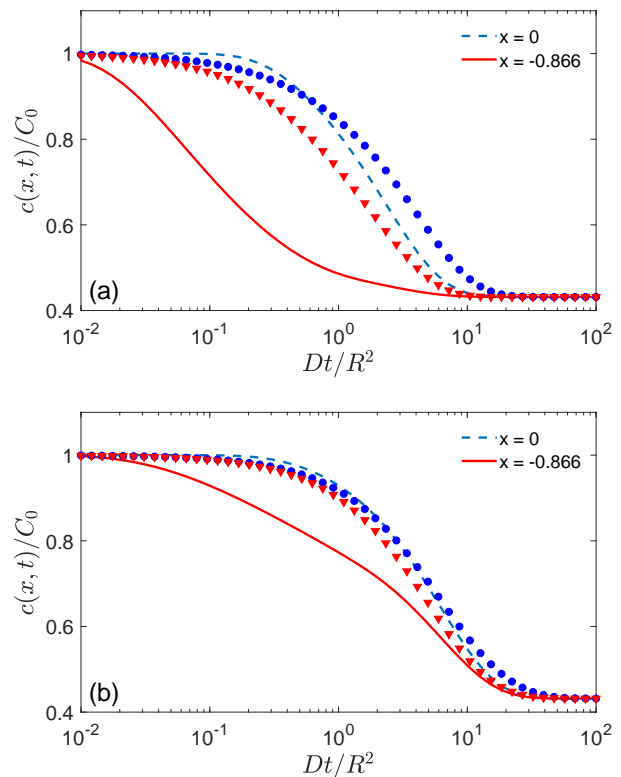


FIG. 3: The normalized concentration $c(x, t)/C_0$ for reversible reactions (with $\mu = 0$) as a function of rescaled time Dt/R^2 , for a target of angular size $\varepsilon = \pi/12$, and two starting points: $x = 0$ (the equator) and $x = \cos(\pi - 2\varepsilon) \approx -0.886$ (close to the target). Lines show the exact solution (34), truncated at $n_{\max} = 20$, while symbols present the approximate solution (60). (a) $\kappa R/D = 10$ and $\lambda R^2/D = 1$; (b) $\kappa R/D = 1$ and $\lambda R^2/D = 0.1$.

F. Small-target asymptotic behavior

In many practical applications, the radius ρ of the target is much smaller than the radius R of the sphere, i.e., $\varepsilon \ll 1$ and a is close -1 . In the conventional first-passage time framework, this situation is known as the narrow escape problem [49, 50]. Here we summarize the asymptotic behavior of our solutions in the narrow escape limit $\varepsilon \rightarrow 0$ (see details in Appendix E).

In the limit $\varepsilon = 0$, a point-like target cannot be accessed by Brownian motion on the sphere and thus corresponds to no target situation, in which the spectrum of the governing operator \mathcal{L} is simply $\nu_n = n$ for $n = 0, 1, 2, \dots$, whereas the eigenfunctions $P_\nu(x)$ are the Legendre polynomials. In particular, the concentration $c(x, t)$ remains constant, whereas the flux $J(t)$ is zero.

When ε is small but nonzero, finding such a small target is a long search process. In Appendix E, we deduce

the long-time behavior of the total flux as

$$J(t) \simeq \frac{4\pi C_0 R^2}{T} e^{-t/T} \quad (t \rightarrow \infty), \quad (61)$$

with a characteristic time T , which is determined by the smallest eigenvalue of the diffusion operator:

$$T = \frac{R^2}{D\nu_0(\nu_0 + 1)} \simeq \frac{R^2}{D\nu_0} \quad (\varepsilon \ll 1). \quad (62)$$

Since the factor $N_B = 4\pi C_0 R^2 \simeq 2\pi(1-a)C_0 R^2$ is simply the total initial number of diffusing particles B , the above expression (61) can be understood as an exponential distribution of the first-passage times for N_B independent particles. The asymptotic behavior of the smallest degree ν_0 was obtained in Appendix E for four different scenarios:

(i) For a perfectly reactive target ($\kappa = \infty$), one gets

$$\nu_0 \simeq \frac{1}{2 \ln(2/\varepsilon)} \quad (\varepsilon \ll 1). \quad (63)$$

The associated time scale $T = 2R^2 \ln(2/\varepsilon)/D$ is close to the mean FPT to a perfectly reactive target (the first term in Eq. (59)), see also [26].

(ii) For irreversible reactions ($\lambda = 0$, $\kappa < \infty$), the smallest degree ν_0 vanishes linearly with ε ,

$$\nu_0 \simeq \frac{\kappa \varepsilon R}{2D} \approx \frac{\kappa \rho}{2D} \quad (\varepsilon \ll 1). \quad (64)$$

The associated time scale $T = 2R^2/(\kappa\rho)$ does not depend on the diffusion coefficient and is close to the mean FPT to a weakly reactive target (the second term in Eq. (59)), see also [27].

(iii) For reversible reactions ($\lambda > 0$, $\mu = 0$), the smallest degree ν_0 is equal to 0 for any target size. In this case, the steady-state total flux is zero, $J(\infty) = 0$, while the steady-state concentration remains close to the initial concentration C_0 :

$$c_\infty \simeq C_0 \left(1 + \frac{\kappa\rho}{2\lambda}\right)^{-1}, \quad (65)$$

as expected. The approach to the steady state is controlled by the next eigenvalue, $\nu_1(\nu_1 + 1) = 2 + O(\varepsilon)$, which sets the time scale $R^2/(2D)$. However, if the dissociation rate λ is small, $\bar{\lambda} < 1$, the approach is controlled by the solution in Eq. (E18), which sets the longer time scale $1/\lambda$.

(iv) For partly reversible reactions ($\lambda > 0$, $\mu > 0$), we obtain (see Appendix E)

$$\nu_0 \simeq \frac{\mu\kappa\rho}{2D(\mu + \lambda)}, \quad (66)$$

which is reduced to the second situation by setting $\lambda = 0$ and to the third situation by setting $\mu = 0$. This value determines the time scale $T = 2R^2(1 + \lambda/\mu)/(\kappa\rho)$.

In analogy to the exact solution (59) for the mean FPT, we propose an interpolation formula for the time scale T :

$$T = \frac{2R^2 \ln(2R/\rho)}{D} + \frac{2R^2(1 + \lambda/\mu)}{\kappa\rho}. \quad (67)$$

In the limit $\kappa = \infty$, one retrieves the time scale for a perfectly reactive target. In turn, for moderate values of κ , the second term provides the dominant contribution in the small-target limit ($\rho \ll R$).

Figure 4(a) illustrates an excellent agreement between numerically computed values of ν_0 and its asymptotic relations. In addition, Fig. 4(b) shows the accuracy of the long-time approximation (61) for a target of angular size $\varepsilon = 0.01$. One can see that our explicit formulas accurately describe the long-time behavior of the total flux toward the target in different regimes.

G. Inclusion of constant flux from the bulk

Our description can be further extended e.g., by incorporating a constant flux of particles from the bulk. In this case, the concentration is constantly fed, and the diffusion equation (3) can be modified by adding the constant flux density J (in units mol/m²/s) to the right-hand side. In the Laplace domain, this is equivalent to changing C_0 to $C_0 + J/s$ in Eq. (14b), as well as in the solutions (27, 28). As a consequence, one gets

$$c_b(x, t) = c(x, t) + \frac{J}{C_0} \int_0^t dt' c(x, t') \quad (68)$$

and

$$J_b(t) = J(t) + \frac{J}{C_0} \int_0^t dt' J(t'), \quad (69)$$

where $c(x, t)$ and $J(t)$ are the former solutions without bulk flux. Substitution of the exact decompositions (34, 36) into Eqs. (68, 69) yields

$$c_b(x, t) = c_b(x, \infty) + C_0 \sum_{n=0}^{\infty} \left[1 - \frac{JR^2}{DC_0\nu_n(\nu_n + 1)} \right] \times c_n P_{\nu_n}(x) e^{-Dt\nu_n(\nu_n+1)/R^2} \quad (70)$$

and

$$J_b(t) = J_b(\infty) + C_0 D \sum_{n=0}^{\infty} \left[1 - \frac{JR^2}{DC_0\nu_n(\nu_n + 1)} \right] \times J_n e^{-Dt\nu_n(\nu_n+1)/R^2}, \quad (71)$$

where

$$c_b(x, \infty) = \frac{JR^2}{D} \sum_{n=0}^{\infty} \frac{c_n}{\nu_n(\nu_n + 1)} P_{\nu_n}(x), \quad (72)$$

$$J_b(\infty) = JR^2 \sum_{n=0}^{\infty} \frac{J_n}{\nu_n(\nu_n + 1)} \quad (73)$$

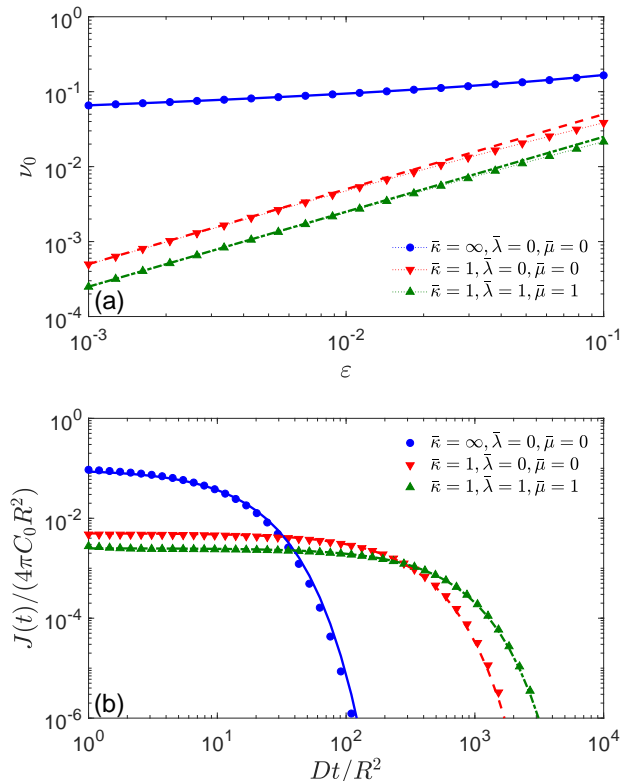


FIG. 4: (a) The smallest degree ν_0 as a function of the target angular size ε , for three configurations of reaction parameters: perfectly reactive target ($\bar{\kappa} = \infty$), partially reactive target with irreversible binding ($\bar{\kappa} = 1, \bar{\lambda} = 0$), and partially reactive target with partly reversible binding ($\bar{\kappa} = 1, \bar{\lambda} = 1, \bar{\mu} = 1$). Symbols show the numerical solutions of Eq. (48) for the first two cases, and of Eq. (30) for the last case. Lines show the asymptotic results (63, 64, 66). (b) The total flux $J(t)$ (normalized by $4\pi C_0 R^2$) as a function of rescaled time Dt/R^2 , for a target of the angular size $\varepsilon = 0.01$, and three configurations of reaction parameters as above. Symbols show the exact solution (36), truncated at $n_{\max} = 20$, while lines present the long-time asymptotic formula (61).

are the steady-state concentration and diffusive flux, respectively. In contrast to the case without bulk flux, the concentration and the diffusive flux do not vanish as $t \rightarrow \infty$ but reach a steady-state regime. Expectedly, this flux does not depend on the diffusion coefficient D , except for the implicit dependence via ν_n . Note that the term $n = 0$ should be treated separately in the case of fully reversible reactions ($\lambda > 0, \mu = 0$), for which $\nu_0 = 0$.

V. CONCLUSIONS AND PERSPECTIVES

In this paper, we investigated diffusion of particles on the surface of a sphere toward a partially reactive target with partly reversible binding kinetics. In this setting, a diffusing particle binds to the target with a certain proba-

bility and then, after some residence time on the target, it can either unbind to resume diffusion, or be transformed into another particle. These reaction mechanisms were characterized by three parameters: the reactivity κ (controlling binding to the target), the dissociation rate λ (controlling unbinding from the target), and the transformation rate μ (controlling the ultimate irreversible chemical transformation). This is a rather general reaction model that englobes most of formerly considered situations. In particular, we distinguished four scenarios: (i) an ideal sink ($\kappa = \infty$; λ does not matter), (ii) a partially reactive target with irreversible binding ($\kappa < \infty$ and $\lambda = 0$), (iii) a partially reactive target with reversible binding and no chemical transformation ($\kappa < \infty, \lambda > 0, \mu = 0$), and (iv) a partially reactive target with reversible binding and chemical transformation ($\kappa < \infty, \lambda > 0, \mu > 0$). Most former studies were dedicated to the first and (less) to the second situation.

Employing the axial symmetry of the problem, we derived the exact solution of the underlying diffusion-reaction equations in terms of Legendre functions. While the case of irreversible reactions on the surface of a sphere was studied in the past [4, 7], the coupling of differential equations for reversible reactions presented a mathematical obstacle in getting an exact solution in time domain. We solved this problem and derived a new equation determining the eigenvalues of the governing diffusion operator. While our solution is valid for any target size, further simplifications were achieved in the small-target limit. Here, we determined the asymptotic behavior of the eigenvalues of the governing operator. In particular, the smallest eigenvalue controls the long-time exponential decay of the total flux. Moreover, we proposed a simple interpolation formula (67) for the time scale T of this decay that includes all the reaction parameters.

While surface diffusion on a cell membrane is an emblematic problem that inspired our work, the proposed method is not limited to cellular biology. For instance, one can think of animal or human migration on Earth, including the problems of epidemic spreading, in which first-passage time phenomena are critically relevant, even though the dynamics of such processes is usually more complex than ordinary diffusion. More generally, this geometric setting allows one to study the effect of curvature onto diffusion-reaction processes, as compared to a flat annulus geometry on the plane. The latter case is simpler and was much more thoroughly studied, especially for irreversible reactions [46, 52–54]. Following the same lines as in Sec. III, one can derive the exact solution describing partly reversible diffusion-influenced reactions (see also [28], in which such a solution was derived for the case $\mu = 0$). A systematic analysis of the curvature effect onto diffusion-reaction processes presents an interesting perspective of this work.

Due to a finite surface area of the sphere and thus a finite amount of diffusing particles, a steady-state solution of the underlying diffusion equation in the presence of a sink is zero, so that one has to look for a transient,

time-dependent solution. Moreover, the passage from the bounded surface on the sphere to the whole plane does not resolve the difficulties [51]. In fact, the recurrent character of Brownian motion implies that there is no steady-state solution in the plane with a finite concentration at infinity. This is in contrast to three-dimensional unbounded domains, for which a nonzero steady-state regime can be reached. In particular, the reaction rate of particles diffusing in \mathbb{R}^3 toward a spherical sink was first computed a century ago by Smoluchowski [55] and then extended to various target configurations (see [56–59] and references therein).

Our exact solution for the concentration of particles revealed limitations of some common practices. In particular, the survival probability of a particle diffusing in a bounded domain toward a target is often approximated by a single exponential function (see [7, 60, 61] and references therein). This is a long-time approximation, which is accurate when the starting point is far from the target or when it is averaged over the whole domain. In both cases, the particle diffuses for long time until its binding to the target and thus can largely explore the whole bounded domain, resulting in such an exponential law. However, if the particle starts relatively close to the target, it can bind to the target very rapidly, on a time scale much shorter than that of the diffusive exploration of the domain [62–64]. As a consequence, the exponential function fails to describe the intricate short-time behavior of the survival probability. This is particularly relevant for reversible reactions because the dissociated particle is released on the target. For instance, we showed in Sec. IV E that the approximation by Prüstel and Tachiya based on the exponential approximation may be accurate for distant starting points but fails if the starting point is close to the target.

The developed description of partly reversible diffusion-influenced reactions is not limited to a spherical shape. It can be easily adapted to general manifolds or Euclidean domains. While the possibility of getting the exact solution strongly relied on the symmetries of the spherical surface, small-target asymptotic results may potentially be derived without knowledge of an exact solution, as it was done for ideal sinks [26, 50] or partially absorbing traps on a cylindrical dendritic membrane [65]. Apart from considering other domains and manifolds, the presented approach can be extended in different directions. First, we showed in Sec. IV G how to incorporate a constant flux density from the bulk and to get stationary solutions. In this way, surface diffusion toward the target can be coupled to bulk diffusion (see also [66] and references therein). The bulk flux may account, e.g., for particles coming from the exterior of a cell membrane or from the interior of the cell. The latter case can model “recycling” of proteins by the cell. Second, one can consider diffusion on a part of the sphere delimited by two circles of latitude. This is equivalent to solving the diffusion-reaction equation (19) for $\tilde{c}(x, s)$ on an interval (a, b) . As previously, the endpoint a corresponds to the target,

whereas the circle of latitude determined by $\cos\theta = b$ can mimic a biological frontier that confines proteins, e.g., in a lipid raft [67–69]. Alternatively, if there are many targets that are more or less uniformly distributed on the surface of a sphere, one can virtually split this surface into “zones of influence” of each target. Even if the particle can cross the virtual border of each zone of influence, such a crossing would simply mean changing the zone of influence and can thus be modeled by reflecting boundary condition. A solution in such a geometric setting would involve Legendre functions of two kinds, $P_\nu(x)$ and $Q_\nu(x)$. The problem with multiple small targets may also be addressed by extending the asymptotic methods developed in [27]. Third, one can investigate first-passage quantities describing multiple independent particles such as, e.g., the first moment when n among N particles are bound to the target. The reversible binding makes these statistics highly nontrivial [70, 71]. Finally, an extension of the proposed formalism beyond Brownian motion presents an important perspective. In fact, single-particle tracking experiments on cell membranes witness considerable deviations from ordinary diffusion [72–74]. Some theoretical models of anomalous diffusion such as continuous-time random walks or processes with diffusing diffusivity can be implemented into our description, at least in Laplace domain (see discussions in [75–78] and references therein).

Acknowledgments

The author acknowledges Prof. D. Calebiro for inspiring discussions.

Appendix A: Some properties of Legendre functions

The Legendre function $P_\nu(x)$ of the first kind is the solution of the Legendre equation (21), which is regular at $x = 1$ and normalized such that $P_\nu(1) = 1$. For an integer ν , $P_\nu(x)$ is the Legendre polynomial of degree ν . In general, the Legendre function is expressed through the hypergeometric function:

$$P_\nu(x) = {}_2F_1(-\nu, \nu + 1; 1; (1 - x)/2), \quad (\text{A1})$$

which is defined as

$${}_2F_1(a, b; c; z) = \sum_{n=0}^{\infty} \frac{(a)_n (b)_n}{(c)_n n!} z^n, \quad (\text{A2})$$

with $(a)_n = a(a + 1) \dots (a + n - 1)$ (and $(a)_0 = 1$). For non-integer ν , the Legendre function $P_\nu(x)$ has a logarithmic divergence at $x = -1$. In turn, for any fixed $x > -1$, $P_\nu(x)$ is an entire analytic function of ν because the hypergeometric series in Eq. (A2) converges uniformly for any finite domain of $\nu \in \mathbb{C}$, see [79] (p.68) for a similar statement for the hypergeometric function. Many properties of the Legendre function are discussed

in the classic textbook by Hobson [80], while their applications in electric potential problems are summarized in [81] (see also [82, 83]). Here we reproduce some properties that are relevant for our work.

Multiplying Eq. (21) by $P_{\nu'}(x)$, subtracting its symmetrized version and integrating over x from a to 1, one immediately deduces

$$\begin{aligned} & \frac{(\nu - \nu')(\nu + \nu' + 1)}{1 - a^2} \int_a^1 dx P_{\nu}(x) P_{\nu'}(x) \quad (\text{A3}) \\ & = P_{\nu'}(a)P'_{\nu}(a) - P_{\nu}(a)P'_{\nu'}(a), \end{aligned}$$

where $P'_{\nu}(a) = (\partial_x P_{\nu}(x))_{x=a}$. In turn, the integral of Eq. (21) from a to 1 yields

$$\int_a^1 dx P_{\nu}(x) = \frac{P_{\nu-1}(a) - P_{\nu+1}(a)}{2\nu + 1} = \frac{1 - a^2}{\nu(\nu + 1)} P'_{\nu}(a), \quad (\text{A4})$$

where we used the recurrence relation

$$(\nu + 1)P_{\nu+1}(x) = (2\nu + 1)xP_{\nu}(x) - \nu P_{\nu-1}(x) \quad (\text{A5})$$

and the expression for the derivative with respect to x :

$$P'_{\nu}(x) = (\nu + 1) \frac{P_{\nu+1}(x) - xP_{\nu}(x)}{x^2 - 1}. \quad (\text{A6})$$

The normalization constants b_n in Eq. (25) can be computed in a standard way. On one hand, the Legendre equation (21) is multiplied by $\partial_{\nu} P_{\nu}(x)$ and integrated over x from a to 1. On the other hand, the Legendre equation is differentiated with respect to ν , multiplied by $P_{\nu}(x)$ and then integrated. Taking the difference of two equations and integrating by parts, one gets

$$\begin{aligned} & \int_a^1 dx [P_{\nu}(x)]^2 = \frac{1}{2\nu + 1} \quad (\text{A7}) \\ & \times \left((1 - x^2) [\partial_{\nu} P_{\nu}(x) P'_{\nu}(x) - P_{\nu}(x) \partial_{\nu} P'_{\nu}(x)] \right) \Big|_{x=a}^{x=1}. \end{aligned}$$

$$P_{\nu}(x) = \frac{\sin(\pi\nu)}{\pi} \left\{ \left[\ln\left(\frac{1+x}{2}\right) + 2\gamma + \psi(\nu + 1) + \psi(-\nu) \right] P_{\nu}(-x) + \sum_{k=1}^{\infty} \frac{(-1)^k \Gamma(\nu + k + 1)}{\Gamma(\nu - k + 1)(k!)^2} \varphi(\nu, k) \left(\frac{1+x}{2}\right)^k \right\}, \quad (\text{A11})$$

where $\psi(\nu) = \frac{d \log \Gamma(\nu)}{d\nu}$ is the digamma function, $\gamma = 0.5772 \dots$ is the Euler constant, and

$$\begin{aligned} \varphi(\nu, k) & = -2 \left(\frac{1}{1} + \dots + \frac{1}{k} \right) + \left(\frac{1}{\nu + 1} + \dots + \frac{1}{\nu + k} \right) \\ & + \left(\frac{1}{-\nu} + \dots + \frac{1}{-\nu + k - 1} \right). \quad (\text{A12}) \end{aligned}$$

Taking the derivative of Eq. (A6) with respect to ν , one finds

$$\partial_{\nu} P'_{\nu}(x) = \frac{P'_{\nu}(x)}{\nu + 1} + \frac{\nu + 1}{x^2 - 1} (\partial_{\nu} P_{\nu+1}(x) - x \partial_{\nu} P_{\nu}(x)), \quad (\text{A8})$$

from which

$$\begin{aligned} & \int_a^1 dx [P_{\nu}(x)]^2 = \frac{1}{2\nu + 1} \left(P_{\nu}(x)(P_{\nu+1}(x) - xP_{\nu}(x)) \right. \\ & \left. + (\nu + 1) [P_{\nu}(x) \partial_{\nu} P_{\nu+1}(x) - P_{\nu+1}(x) \partial_{\nu} P_{\nu}(x)] \right) \Big|_{x=a}^{x=1}. \end{aligned}$$

Since $P_{\nu}(1) = 1$, the normalization coefficients b_n in Eq. (25) are obtained from

$$\begin{aligned} & \int_a^1 dx [P_{\nu}(x)]^2 = \frac{-1}{2\nu + 1} \left(P_{\nu}(a)(P_{\nu+1}(a) - aP_{\nu}(a)) \right. \\ & \left. + (\nu + 1) [P_{\nu}(a) \partial_{\nu} P_{\nu+1}(a) - P_{\nu+1}(a) \partial_{\nu} P_{\nu}(a)] \right). \quad (\text{A9}) \end{aligned}$$

For Dirichlet boundary condition $P_{\nu}(a) = 0$, one recovers the relation from [81]:

$$\int_a^1 dx [P_{\nu}(x)]^2 = -\frac{1 - a^2}{2\nu + 1} \left(\partial_{\nu} P_{\nu}(x) P'_{\nu}(x) \right)_{x=a}. \quad (\text{A10})$$

Some approximate formulas for computing $\partial_{\nu} P_{\nu}(a)$ were also provided in that reference.

Hobson derived the following representation of $P_{\nu}(x)$ for negative x [80]:

Schelkunoff gave approximate expressions for Legendre functions of nearly integral degree [84], e.g.,

$$P_{\epsilon}(x) \simeq 1 + \epsilon \ln\left(\frac{1+x}{2}\right), \quad (\text{A13a})$$

$$P_{1+\epsilon}(x) \simeq x + \epsilon \left[x - 1 + x \ln\left(\frac{1+x}{2}\right) \right], \quad (\text{A13b})$$

which are applicable for all $|x| < 1$ and yield an error of the order of ϵ^2 .

To compute Legendre functions numerically at large ν , it is convenient to use the Mehler-Dirichlet integral representation

$$P_\nu(\cos \theta) = \frac{\sqrt{2}}{\pi} \int_0^\theta d\alpha \frac{\cos((\nu + 1/2)\alpha)}{\sqrt{\cos \alpha - \cos \theta}}, \quad (\text{A14})$$

which is valid for $\theta \in (0, \pi)$ and $\nu \in \mathbb{C}$ [80]. From this representation, one can also evaluate

$$\partial_\nu P_\nu(\cos \theta) = -\frac{\sqrt{2}}{\pi} \int_0^\theta d\alpha \frac{\alpha \sin((\nu + 1/2)\alpha)}{\sqrt{\cos \alpha - \cos \theta}}. \quad (\text{A15})$$

These two relations were used throughout this paper for numerical computations of $P_\nu(x)$ and $\partial_\nu P_\nu(x)$.

Note that the derivative of the Legendre function with respect to its degree can also be written as [87–89]:

$$\partial_\nu P_\nu(x) = \pi \tan(\pi \nu) P_\nu(x) - \frac{1}{\pi} A_\nu(x), \quad (\text{A16})$$

where

$$A_\nu(x) = \sin(\pi \nu) \sum_{k=0}^{\infty} \frac{((1-x)/2)^k \Gamma(k-\nu) \Gamma(k+\nu+1)}{(k!)^2} \times (\psi(k+\nu+1) - \psi(k-\nu)). \quad (\text{A17})$$

One also gets

$$\partial_\nu P'_\nu(a) = \frac{P'_\nu(a)}{\nu+1} + \frac{\nu+1}{a^2-1} [\partial_\nu P_{\nu+1}(a) - a \partial_\nu P_\nu(a)]. \quad (\text{A18})$$

However, these relations are less convenient than the integral presentation (A15) for numerical computations.

Appendix B: Spectral properties

1. Solutions ν_n^s of Eq. (22)

If ν and ν' denote any two solutions of Eq. (22) (with a fixed q_s), the right-hand side of Eq. (A3) is zero, ensuring the orthogonality of the corresponding Legendre functions. This property holds for Neumann ($q_s = 0$), Robin ($0 < q_s < \infty$) and Dirichlet ($q_s = \infty$) boundary conditions.

Moreover, MacDonald used Eq. (A3) to prove that all zeros of $P_\nu(a)$ are real [86] (see also an amendment to the proof in [80]). His argument can be directly applied to prove that all zeros of $P'_\nu(a) - q_s P_\nu(a)$ are also real for any fixed real q_s . It is enough to rewrite the right-hand side of Eq. (A3) as

$$\frac{1}{q_s} \left([q_s P_{\nu'}(a) - P'_{\nu'}(a)] P'_\nu(a) - [q_s P_\nu(a) - P'_\nu(a)] P'_{\nu'}(a) \right).$$

If ν was a complex zero of $P'_\nu(a) - q_s P_\nu(a)$, then its complex conjugate, $\nu' = \nu^*$, would also be a zero (given that $P_{\nu^*}(a) = P_\nu^*(a)$), implying that the integral in Eq. (A3) would vanish. This is not possible because $P_\nu(x) P_{\nu'}(x) = |P_\nu(x)|^2$ for such a pair of complex conjugate degrees ν and ν' (see [80] for details).

As $P_\nu(x)$ is an entire analytic function of ν for any fixed $x > -1$ (see Appendix A), whereas ν^s is a solution of Eq. (22) involving $P_\nu(a)$ and $P'_\nu(a)$, we expect that $P_{\nu^s}(x)$ as a function of s has no poles. A rigorous proof of this claim is beyond the scope of this paper.

2. Solutions ν_n of Eq. (30)

The above arguments are not directly applicable for the solutions ν_n of Eq. (30). In fact, rewriting again the right-hand side of Eq. (A3) in a form that is consistent with Eq. (30), one gets

$$\begin{aligned} & \frac{(\nu - \nu')(\nu + \nu' + 1)}{1 - a^2} \int_a^1 dx P_\nu(x) P_{\nu'}(x) \\ &= P'_\nu(a) \left(P_{\nu'}(a) - \frac{\bar{\lambda} + \bar{\mu} - \nu'(\nu' + 1)}{q(\bar{\mu} - \nu'(\nu' + 1))} P'_{\nu'}(a) \right) \\ & - P'_{\nu'}(a) \left(P_\nu(a) - \frac{\bar{\lambda} + \bar{\mu} - \nu(\nu + 1)}{q(\bar{\mu} - \nu(\nu + 1))} P'_\nu(a) \right) \\ & - \frac{\bar{\lambda}(\nu - \nu')(\nu + \nu' + 1)}{q(\bar{\mu} - \nu(\nu + 1))(\bar{\mu} - \nu'(\nu' + 1))} P'_\nu(a) P'_{\nu'}(a). \end{aligned}$$

If ν and ν' are any two solutions of Eq. (30), the first two terms on the right-hand side vanish, but the last term does not. As a consequence, the functions $P_\nu(x)$ and $P_{\nu'}(x)$, as well as all $P_{\nu_n}(x)$, determining $c(x, t)$ and $J(t)$ via Eqs. (34, 36), are not orthogonal to each other.

At the same time, the above relation still allows us to prove that all solutions of Eq. (30) are real. If there existed a complex solution ν , then its complex conjugate, $\nu' = \nu^*$, would also be a solution so that the above relation would become

$$\int_a^1 dx |P_\nu(x)|^2 = -\frac{\bar{\lambda}(1 - a^2) |P'_\nu(a)|^2}{q |\bar{\mu} - \nu(\nu + 1)|^2}.$$

However, this relation cannot hold because the left-hand side is the integral of a positive function, whereas the right-hand side is negative.

3. Computation of the residues

The Laplace inversion formulas include the factor $(\partial_s f_n)(s_n)$ which can be written as

$$\partial_s f_n(s_n) = 1 + \frac{D}{R^2} (2\nu_n + 1) (\partial_s \nu_n)(s_n), \quad (\text{B1})$$

where ν_n is a shortcut notation for $\nu_n^{s_n}$, i.e., the n -th solution of Eq. (22) evaluated at the pole s_n . The last factor can be found by differentiating the boundary condition (22):

$$\partial_s \nu_n(s_n) = \frac{\bar{\kappa} \lambda P_{\nu_n}(a) \left(\partial_\nu P'_\nu(a) - q_{s_n} \partial_\nu P_\nu(a) \right)_{\nu=\nu_n}^{-1}}{\sqrt{1-a^2}(s_n + \lambda + \mu)^2}, \quad (\text{B2})$$

so that one needs to evaluate the derivative with respect to the degree ν . Using Eqs. (A16, A18) and the boundary condition (22), one gets

$$\begin{aligned} \left(\partial_\nu P'_\nu(a) - q_{s_n} \partial_\nu P_\nu(a) \right)_{\nu=\nu_n} &= \frac{P'_{\nu_n}(a)}{\nu_n + 1} \\ &- \frac{1}{\pi} \left[\frac{\nu_n + 1}{a^2 - 1} (A_{\nu_n+1}(a) - a A_{\nu_n}(a)) - q_{s_n} A_{\nu_n}(a) \right]. \end{aligned} \quad (\text{B3})$$

In practice, we used the integral representation (A15) for evaluating Eq. (B2).

4. Estimates for zeros ν_n^s

We discuss some properties of the solutions ν_n^s of Eq. (22) (with fixed a and q_s) that may facilitate their numerical computation. Even though most of the following statements are expected to be classical, we could not find their mathematical proofs in the literature. As such proofs are beyond the scope of the paper, most of the results of this section of the Appendix remain conjectural from the mathematical point of view, even so they have been checked numerically. We emphasize that the conjectural results of this section were not directly used in the main text, except for guiding the author in the analysis. As a consequence, their conjectural character does not impair the quality of main results. In the following, we assume that $q_s \geq 0$.

Since the operator $\mathcal{L} = \partial_x(1-x^2)\partial_x$ is self-adjoint, the minimax principle should imply the standard inequalities between Dirichlet, Robin, and Neumann eigenvalues (see [90, 91] for the case of the Laplace operator in Euclidean domains), from which

$$\nu_n^N \leq \nu_n^s \leq \nu_n^D, \quad (\text{B4})$$

where ν_n^D and ν_n^N are the zeros corresponding to the limiting cases of Dirichlet ($q_s = \infty$) and Neumann ($q_s = 0$) conditions:

$$P_{\nu_n^D}(a) = 0, \quad P'_{\nu_n^N}(a) = 0. \quad (\text{B5})$$

We also expect that ν_n^s are monotonous functions of a :

$$n = \nu_n^s(-1) \leq \nu_n^s(a_1) \leq \nu_n^s(a_2) \quad (a_1 < a_2). \quad (\text{B6})$$

Using the asymptotic expansions of the Legendre function at large ν [85]

$$\begin{aligned} P_\nu(\cos \theta) &= \frac{\Gamma(\nu+1)}{\Gamma(\nu+3/2)} \left(\frac{\pi \sin \theta}{2} \right)^{-1/2} \\ &\times \cos((\nu+1/2)\theta - \pi/4) + O(\nu^{-1}), \end{aligned} \quad (\text{B7})$$

we get

$$\nu_n^D \simeq \nu_n^{D,\text{app}} = \frac{n+3/4}{1-\varepsilon/\pi} - \frac{1}{2} \quad (n \rightarrow \infty), \quad (\text{B8})$$

where we used $\arccos(a) = \pi - \varepsilon$. Note that this asymptotic relation is exact for $a = 0$ (or $\varepsilon = \pi/2$): $\nu_n^D = 2n+1$. We conjecture that for all $n = 0, 1, 2, \dots$,

$$\nu_n^D \leq \nu_n^{D,\text{app}} \quad (a < 0), \quad (\text{B9a})$$

$$\nu_n^D \geq \nu_n^{D,\text{app}} \quad (a > 0). \quad (\text{B9b})$$

In other words, the asymptotic approximation $\nu_n^{D,\text{app}}$ is either the upper bound (for $a < 0$), or the lower bound (for $a > 0$) for the zeros ν_n^D . These inequalities have been checked numerically for several values of a and n .

Similarly, taking the derivative of $P_\nu(x)$ with respect to x , one gets

$$\begin{aligned} P'_\nu(\cos \theta) &= \frac{\pi}{2} \frac{\Gamma(\nu+2)}{\Gamma(\nu+3/2)} \left(\frac{\pi \sin \theta}{2} \right)^{-3/2} \\ &\times \sin((\nu+1/2)\theta - \pi/4) + O(\nu^{-1}), \end{aligned} \quad (\text{B10})$$

so that

$$\nu_n^N \simeq \nu_n^{N,\text{app}} = \frac{n+1/4}{1-\varepsilon/\pi} - \frac{1}{2} \quad (n \rightarrow \infty). \quad (\text{B11})$$

This asymptotic relation becomes exact for $a = 0$ (or $\varepsilon = \pi/2$): $\nu_n^N = 2n$. We conjecture that for all $n = 0, 1, 2, \dots$,

$$\nu_n^N \geq \nu_n^{N,\text{app}} \quad (a < 0), \quad (\text{B12a})$$

$$\nu_n^N \leq \nu_n^{N,\text{app}} \quad (a > 0). \quad (\text{B12b})$$

In other words, the asymptotic approximation $\nu_n^{N,\text{app}}$ is either the lower bound (for $a < 0$), or the upper bound (for $a > 0$) for the zeros ν_n^N . These inequalities have been checked numerically for several values of a and n .

Combining these inequalities with Eq. (B4), we get the following conjectural inequalities for $a < 0$:

$$\nu_n^{N,\text{app}} \leq \nu_n^N \leq \nu_n^s \leq \nu_n^D \leq \nu_n^{D,\text{app}}. \quad (\text{B13})$$

We note that the case $a < 0$ (small targets) is more relevant for applications than $a > 0$ (large targets). These inequalities allow one to impose constraints on the range of ν , on which the n -th zero ν_n^s is searched numerically. At $n = 0$, the lower bound is negative and should thus be replaced by 0.

Appendix C: Example of numerical implementation

In this Appendix, we illustrate the computation of the total flux $J(t)$ shown in Fig. 4(b). After truncation of the spectral decomposition (36) at $n_{\max} = 20$, this flux is approximated by 20 exponential functions, determined by ν_n and J_n , with $n = 0, 1, 2, \dots, 19$. For a given set of dimensionless parameters (ε , $\bar{\kappa}$, $\bar{\lambda}$, and $\bar{\mu}$), we first determined ν_n by solving Eq. (30) by a bisection method; then the coefficients J_n were computed from Eq. (37), as discussed in Sec. IV D.

Figure 5 shows the first 20 parameters ν_n and J_n that were used for plotting Fig. 4(b) for a small target $\varepsilon = 0.01$ and three configurations of reaction parameters. For convenience, ν_n are divided by $n + 1$, to highlight their asymptotic behavior $\nu_n \propto n$. In all three cases, the smallest solution ν_0 is small but strictly positive (its dependence on ε was shown in Fig. 4(a)). As n increases, $\nu_n/(n+1)$ approaches 1 from below, suggesting that $n+1$ is the upper bound of ν_n . Even though a rigorous proof of this statement is beyond the scope of the paper (see also Appendix B 4), one can use the relation $\nu_n \propto n$ to estimate the validity range of the truncated decomposition. In fact, the omission of the terms with $n \geq n_{\max}$ is justified when $Dt\nu_n(\nu_n + 1)/R^2 \gg 1$, i.e., $Dt/R^2 \gg n_{\max}^{-2}$. This inequality is satisfied for all figures in the paper.

For the considered three cases of reaction parameters, the coefficients J_n are positive and decreasing with n . The first coefficient J_0 provides the dominant contribution to the total flux, particularly for the case of a partial sink with irreversible reaction ($\bar{\kappa} = 1$, $\bar{\lambda} = \bar{\mu} = 0$).

Appendix D: Derivation of the MFPT

The mean FPT to a partially reactive target on the surface of a sphere was found in [7]. Here we reproduce its computation for the sake of completeness. The MFPT $\tau(x)$ obeys the Poisson equation: $D\Delta\tau = -1$ that reads as

$$\partial_x(1-x^2)\partial_x\tau(x) = -\frac{R^2}{D} \quad (a < x < 1), \quad (\text{D1})$$

subject to the Robin boundary condition at $x = a$: $\frac{D}{R}\sin\varepsilon(\partial_x\tau)(a) = \kappa\tau(a)$. A general solution is obtained by integrating twice the above equation:

$$\tau(x) = \frac{R^2}{2D}\ln(1-x^2) + \frac{c_1}{2}\ln\frac{1+x}{1-x} + c_2, \quad (\text{D2})$$

with two constants c_1 and c_2 . To ensure the regularity of this solution at $x = 1$, we set $c_1 = R^2/D$ so that

$$\tau(x) = \frac{R^2}{D}\ln(1+x) + c_2. \quad (\text{D3})$$

The constant c_2 is fixed by the Robin boundary condition, from which Eq. (59) follows.

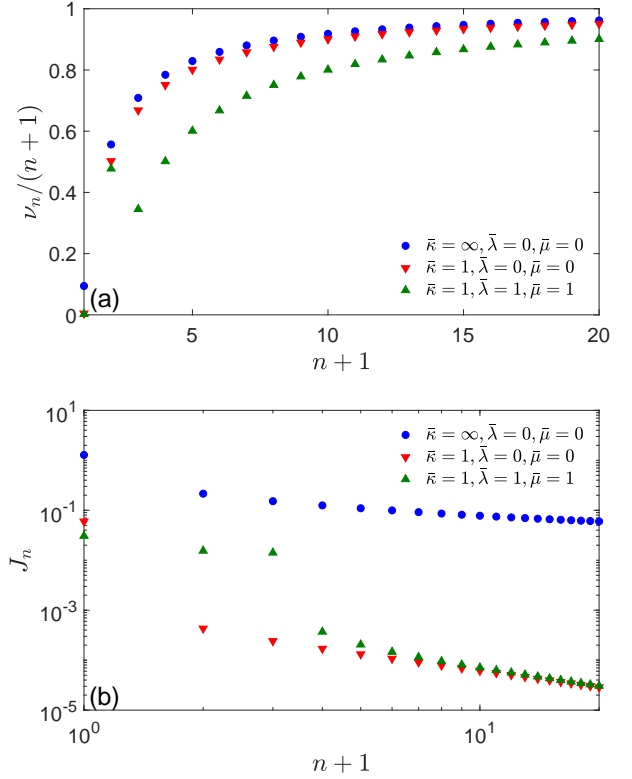


FIG. 5: Parameters used to plot Fig. 4(b) with $\varepsilon = 0.01$ for three configurations of reaction parameters: perfectly reactive target ($\bar{\kappa} = \infty$), partially reactive target with irreversible binding ($\bar{\kappa} = 1$, $\bar{\lambda} = 0$), and partially reactive target with partly reversible binding ($\bar{\kappa} = 1$, $\bar{\lambda} = 1$, $\bar{\mu} = 1$). (a) The first 20 solutions ν_n of Eq. (30), divided by $n + 1$ for convenience. (b) The first 20 coefficients J_n in Eq. (36) for the total flux $J(t)$.

Appendix E: Asymptotic behavior for small targets

In this Appendix, we investigate separately the asymptotic behavior of the solutions ν_n^s of Eq. (22) and that of the solutions ν_n of Eq. (30) in the limit $\varepsilon \rightarrow 0$.

1. Solutions ν_n^s of Eq. (22)

Here we analyze the asymptotic behavior of the solutions ν_n^s of Eq. (22) for a fixed q_s .

For small ε , we have $a \simeq -1 + \varepsilon^2/2$. Using the Hobson's representation (A11) and $P_\nu(-a) = P_\nu(1 - \varepsilon^2/2) = 1 + O(\varepsilon^2)$, we get

$$P_\nu(a) \simeq \frac{\sin(\pi\nu)}{\pi} \Psi_\varepsilon(\nu) + O(\varepsilon^2), \quad (\text{E1})$$

with

$$\Psi_\varepsilon(\nu) = \ln(\varepsilon^2/4) + 2\gamma + 2\psi(\nu + 1) + \pi\text{ctan}(\pi\nu), \quad (\text{E2})$$

where we used the reflection property of the digamma function: $\psi(1+z) - \psi(-z) = -\pi \cotan(\pi z)$. Substituting this expression into Eq. (51) (which is equivalent to Eq. (22)), we get

$$\pi \cotan(\pi \nu) + 2\psi(\nu+1) \simeq \frac{2}{q_s \varepsilon^2} + 2 \ln(2/\varepsilon) - 2\gamma, \quad (\text{E3})$$

where we used that $\psi(z+1) = \psi(z) + 1/z$. Since the right-hand side of this relation is large as $\varepsilon \rightarrow 0$, ν should lie near the poles of $\cotan(\pi \nu)$. We search thus an approximate solution of Eq. (E3) as

$$\nu_n^s \simeq n + \delta_n, \quad \delta_n \ll 1. \quad (\text{E4})$$

Note that $\psi(\nu+1)$ is regular at positive integers: $\psi(n+1) = H_n - \gamma$, where $H_n = 1/1 + \dots + 1/n$ are the harmonic numbers (and $H_0 = 0$). One gets thus

$$\frac{1}{\delta_n} \simeq \frac{2}{q_s \varepsilon^2} + 2 \ln(2/\varepsilon) - 2H_n. \quad (\text{E5})$$

This approximate solution is valid only when the right-hand side is large (and δ_n is small), yielding a constraint of having not too large n .

In what follows, we will need to evaluate $P'_{\nu_n^s}(a)$. Using again Eq. (A11), we find in the leading term

$$P'_{\nu_n^s}(a) \simeq \frac{\sin(\pi \nu_n)}{\pi(1+a)} \simeq \frac{2\delta_n}{1-a^2}. \quad (\text{E6})$$

Using Eqs. (B1, B2, B3) and representations (A16, A18), we also determine

$$(\partial_s f_n)(s_n) \simeq 1 \quad (\varepsilon \rightarrow 0). \quad (\text{E7})$$

Finally, given that $b_n^2 = n + 1/2$ for $\varepsilon = 0$, this relation should hold approximately for small ε .

In the following, we consider separately the cases of perfect ($\kappa = \infty$) and imperfect ($\kappa < \infty$) target.

Perfect sink

For a perfect sink ($\kappa = \infty$), one has $q_s = \infty$, and the first term in Eq. (E5) vanishes, so that one retrieves the asymptotic formula for the zeros of the Legendre function from Ref. [81]:

$$\nu_n^s = \nu_n \simeq n + \frac{1}{2 \ln(2/\varepsilon) - 2H_n}. \quad (\text{E8})$$

For $n > 0$, the logarithmic term provides a small correction and can thus be neglected so that $\nu_n \simeq n$. In contrast, when $n = 0$, the logarithmic term dominates. One gets thus the asymptotic behavior of $\tilde{c}(x, s)$ and $\tilde{J}(s)$ via Eqs. (27, 28).

Moreover, as q_s is infinite (and thus does not depend on s), the degrees ν_n determine directly the poles via Eq. (33). In particular, one gets

$$s_0 \simeq -\frac{D}{2R^2 \ln(2/\varepsilon)}. \quad (\text{E9})$$

Note that $1/|s_0|$ is close to the mean first passage time to the target in this domain (see Appendix D). Substituting these results into Eq. (36), we get the long-time behavior (61) of the total flux.

Imperfect sink

For imperfect sink ($\kappa < \infty$), one can neglect the logarithmic and constant terms in Eq. (E5), so that

$$\nu_n^s \simeq n + \frac{\bar{\kappa}(s+\mu)}{2(s+\lambda+\mu)} \varepsilon + o(\varepsilon). \quad (\text{E10})$$

This asymptotic relation determines $\tilde{c}(x, s)$ and $\tilde{J}(s)$ via Eqs. (27, 28).

Moreover, for irreversible reactions with $\lambda = 0$, q_s and thus ν_n^s do not depend on s (and μ) so that one can use the above relation to determine the asymptotic behavior of $c(x, t)$ and $J(t)$ in Eqs. (34, 36). In fact, Eq. (33) yields

$$s_n = -\frac{D}{R^2} \left(n(n+1) + (n+1/2)\varepsilon\bar{\kappa} + O(\varepsilon^2) \right). \quad (\text{E11})$$

In a first approximation, one can neglect ε in the higher-order eigenmodes. Keeping only the term with $n = 0$ with the smallest rate $|s_0|$, we get the long-time behavior (61) of the total flux.

2. Solutions ν_n of Eq. (30)

For reversible reactions (with $\lambda > 0$), $c(x, t)$ and $J(t)$ are determined by the solutions ν_n of Eq. (30). To get their asymptotic behavior in the small-target limit, we rewrite Eq. (30) as

$$\bar{\lambda} + \bar{\mu} - \nu(\nu+1) = \bar{\kappa}(\bar{\mu} - \nu(\nu+1)) \frac{P_\nu(a)}{\sqrt{1-a^2} P'_\nu(a)}. \quad (\text{E12})$$

The Hobson representation (A11) for $P_\nu(a)$ and its derivative $P'_\nu(a)$ yields in the limit $\varepsilon \rightarrow 0$:

$$\bar{\lambda} + \bar{\mu} - \nu(\nu+1) = \varepsilon \frac{\bar{\kappa}(\bar{\mu} - \nu(\nu+1)) [\Psi_\varepsilon(\nu) + O(\varepsilon^2)]}{2 + \varepsilon^2 \frac{\nu(\nu+1)}{2} \Psi_\varepsilon(\nu) + O(\varepsilon^2)}, \quad (\text{E13})$$

with $\Psi_\varepsilon(\nu)$ given by Eq. (E2). As the function $\Psi(\nu)$ diverges at any integer ν , one can search again for solutions near integers, $\nu_n = n + \delta_n$, from which

$$\Psi_\varepsilon(\nu_n) = \frac{1}{\delta_n} + \ln(\varepsilon^2/4) + 2H_n + O(\delta) \quad (\text{E14})$$

and thus

$$\delta_n \simeq \frac{\bar{\kappa}(\bar{\mu} - n(n+1))}{2(\bar{\lambda} + \bar{\mu} - n(n+1))} \varepsilon + o(\varepsilon). \quad (\text{E15})$$

For instance, one gets the following asymptotic relation for the smallest degree:

$$\nu_0 = \delta_0 \approx \frac{\bar{\kappa} \bar{\mu} \varepsilon}{2(\bar{\mu} + \bar{\lambda})} \approx \frac{\mu \kappa \rho}{2D(\mu + \lambda)}. \quad (\text{E16})$$

In the particular case when $\bar{\lambda} + \bar{\mu} = n'(n' + 1)$ for some integer n' , Eq. (E15) does not hold for this n' , and one gets a slower approach to the limit:

$$\delta_{n'} \simeq \left(\frac{\bar{\kappa} \bar{\lambda}}{2(2n' + 1)} \right)^{1/2} \sqrt{\varepsilon} + o(\sqrt{\varepsilon}). \quad (\text{E17})$$

Yet another solution of Eq. (E13) is possible when its left-hand side is of the order of ε and the corresponding

ν is not close to an integer. In this case, $\Psi_\varepsilon(\nu)$ behaves asymptotically as $2 \ln(\varepsilon/2) + O(1)$ and thus one gets the solution in the leading order in ε :

$$\nu(\nu + 1) = \bar{\lambda} + \bar{\mu} - \bar{\kappa} \bar{\lambda} \varepsilon \ln(1/\varepsilon) + O(\varepsilon). \quad (\text{E18})$$

As a consequence, the degree ν approaches the value $\sqrt{1/4 + \bar{\lambda} + \bar{\mu}} - 1/2$ in the limit $\varepsilon \rightarrow 0$. We recall that this value should not be integer (otherwise the relation (E18) does not necessarily hold). This solution yields the eigenvalue, which is close to $\bar{\lambda} + \bar{\mu}$. We emphasize that the above argument is not applicable when $\lambda = 0$, in which case q_s does not depend on s any more.

-
- [1] B. Alberts, A. Johnson, J. Lewis, D. Morgan, M. Raff, K. Roberts, and P. Walter, *Molecular Biology of the Cell* (Garland Science, New York, NY, 2014).
- [2] T. Sungkaworn, M.-L. Jobin, K. Burnecki, A. Weron, M. J. Lohse, and D. Calebiro, “Single-molecule imaging reveals receptor-G protein interactions at cell surface hot spots”, *Nature* **550**, 543-547 (2017).
- [3] V. A. Bloomfield and S. Prager, “Diffusion-controlled reactions on spherical surfaces. Application to bacteriophage tail fiber attachment”, *Biophys. J.* **27**, 447-453 (1979).
- [4] N. Chao, S. H. Young, and M. Poo, “Localization of Cell Membrane Components by Surface Diffusion into a Trap”, *Biophys. J.* **36**, 139-153 (1981).
- [5] D. L. Weaver, “Diffusion-mediated localization on membrane surfaces”, *Biophys. J.* **41**, 81-86 (1983).
- [6] J. J. Linderman and D. A. Lauffenburger, “Analysis of intracellular receptor/ligand sorting. Calculation of mean surface and bulk diffusion times within a sphere”, *Biophys. J.* **50**, 295-305 (1986).
- [7] H. Sano and M. Tachiya, “Theory of diffusion-controlled reactions on spherical surfaces and its application to reactions on micellar surfaces”, *J. Chem. Phys.* **75**, 2870 (1981).
- [8] O. G. Berg, “Orientation constraints in diffusion-limited macromolecular association. The role of surface diffusion as a rate-enhancing mechanism”, *Biophys. J.* **47**, 1 (1985).
- [9] O. Bénichou, D. S. Grebenkov, P. Levitz, C. Loverdo, and R. Voituriez, “Optimal Reaction Time for Surface-Mediated Diffusion”, *Phys. Rev. Lett.* **105**, 150606 (2010).
- [10] O. Bénichou, D. S. Grebenkov, P. Levitz, C. Loverdo, and R. Voituriez, “Mean First-Passage Time of Surface-Mediated Diffusion in Spherical Domains”, *J. Stat. Phys.* **142**, 657-685 (2011).
- [11] F. Rojo and C. E. Budde, “Enhanced diffusion through surface excursion: A master-equation approach to the narrow-escape-time problem”, *Phys. Rev. E* **84**, 021117 (2011).
- [12] J.-F. Rupprecht, O. Bénichou, D. S. Grebenkov, and R. Voituriez, “Kinetics of Active Surface-Mediated Diffusion in Spherically Symmetric Domains”, *J. Stat. Phys.* **147**, 891-918 (2012).
- [13] J.-F. Rupprecht, O. Bénichou, D. S. Grebenkov, and R. Voituriez, “Exact mean exit time for surface-mediated diffusion”, *Phys. Rev. E* **86**, 041135 (2012).
- [14] H. C. Berg and E. M. Purcell, “Physics of chemoreception”, *Biophys. J.* **20**, 193-239 (1977).
- [15] R. Zwanzig, “Diffusion-controlled ligand binding to spheres partially covered by receptors: an effective medium treatment”, *Proc. Natl. Acad. Sci. USA* **87**, 5856 (1990).
- [16] R. Zwanzig and A. Szabo, “Time dependent rate of diffusion-influenced ligand binding to receptors on cell surfaces”, *Biophys. J.* **60**, 671 (1991).
- [17] A. Berezhkovskii, Y. Makhnovskii, M. Monine, V. Zitserman, and S. Shvartsman, “Boundary homogenization for trapping by patchy surfaces”, *J. Chem. Phys.* **121**, 11390 (2004).
- [18] A. M. Berezhkovskii, M. I. Monine, C. B. Muratov, and S. Y. Shvartsman, “Homogenization of boundary conditions for surfaces with regular arrays of traps”, *J. Chem. Phys.* **124**, 036103 (2006).
- [19] C. Muratov and S. Shvartsman, “Boundary homogenization for periodic arrays of absorbers”, *Multiscale Model. Simul.* **7**, 44-61 (2008).
- [20] L. Dagdug, M. Vázquez, A. Berezhkovskii, and V. Zitserman, “Boundary homogenization for a sphere with an absorbing cap of arbitrary size”, *J. Chem. Phys.* **145**, 214101 (2016).
- [21] A. E. Lindsay, A. J. Bernoff, and M. J. Ward, “First Passage Statistics for the Capture of a Brownian Particle by a Structured Spherical Target with Multiple Surface Traps”, *Multiscale Model. Simul.* **15**, 74-109 (2017).
- [22] A. J. Bernoff and A. E. Lindsay, “Numerical approximation of diffusive capture rates by planar and spherical surfaces with absorbing pores”, *SIAM J. Appl. Math.* **78**, 266-290 (2018).
- [23] A. Bernoff, A. Lindsay, and D. Schmidt, “Boundary Homogenization and Capture Time Distributions of Semipermeable Membranes with Periodic Patterns of Reactive Sites”, *Multiscale Model. Simul.* **16**, 1411-1447 (2018).
- [24] D. Shoup, G. Lipari, and A. Szabo, “Diffusion-controlled bimolecular reaction rates. The effect of rotational diffu-

- sion and orientation constraints”, *Biophys. J.* **36**, 697-714 (1981).
- [25] D. S. Grebenkov and G. Oshanin, “Diffusive escape through a narrow opening: new insights into a classic problem”, *Phys. Chem. Chem. Phys.* **19**, 2723-2739 (2017).
- [26] A. Singer, Z. Schuss, and D. Holcman, “Narrow Escape, Part III Riemann surfaces and non-smooth domains”, *J. Stat. Phys.* **122**, 491-509 (2006).
- [27] D. Coombs, R. Straube, and M. J. Ward, “Diffusion on a Sphere with Localized Traps: Mean First Passage Time, Eigenvalue Asymptotics, and Fekete Points”, *SIAM J. Appl. Math.* **70**, 302 (2009).
- [28] T. Prüstel and M. Tachiya, “Reversible diffusion-influenced reactions of an isolated pair on some two dimensional surfaces”, *J. Chem. Phys.* **139**, 194103 (2013).
- [29] M. Filoche and B. Sapoval, “Can One Hear the Shape of an Electrode? II. Theoretical Study of the Laplacian Transfer”, *Eur. Phys. J. B* **9**, 755-763 (1999).
- [30] D. S. Grebenkov, M. Filoche, and B. Sapoval, “Spectral Properties of the Brownian Self-Transport Operator”, *Eur. Phys. J. B* **36**, 221-231 (2003).
- [31] D. S. Grebenkov, *Partially Reflected Brownian Motion: A Stochastic Approach to Transport Phenomena*, in “Focus on Probability Theory”, Ed. L. R. Velle, pp. 135-169 (Nova Science Publishers, 2006).
- [32] D. S. Grebenkov, “Residence times and other functionals of reflected Brownian motion”, *Phys. Rev. E* **76**, 041139 (2007).
- [33] A. Singer, Z. Schuss, Osipov, and D. Holcman, “Partially Reflected Diffusion”, *SIAM J. Appl. Math.* **68**, 844 (2008).
- [34] D. Shoup and A. Szabo, “Role of diffusion in ligand binding to macromolecules and cell-bound receptors”, *Biophys. J.* **40**, 33 (1982).
- [35] D. A. Lauffenburger and J. Linderman, *Receptors: Models for Binding, Trafficking, and Signaling* (Oxford University Press, 1993).
- [36] N. Agmon and A. Szabo, “Theory of reversible diffusion-influenced reactions”, *J. Chem. Phys.* **92**, 5270 (1990).
- [37] M. Tachiya, “Theory of diffusion-controlled dissociation and its applications to charge separation,” in Extended Abstract of Annual Meeting on Photochemistry, Tsu, Japan, 1980 (Japan. Photochem. Assoc., 1980), pp. 256-257.
- [38] N. Agmon, “Diffusion with back reaction”, *J. Chem. Phys.* **81**, 2811 (1984).
- [39] H. Kim and K. J. Shin, “Exact Solution of the Reversible Diffusion-Influenced Reaction for an Isolated Pair in Three Dimensions”, *Phys. Rev. Lett.* **82**, 1578 (1999).
- [40] F. C. Goodrich, “Random walk with semi-adsorbing barrier”, *J. Chem. Phys.* **22**, 588-594 (1954).
- [41] F. C. Collins and G. E. Kimball, “Diffusion-controlled reaction rates”, *J. Coll. Sci.* **4**, 425 (1949).
- [42] H. Sano and M. Tachiya, “Partially diffusion-controlled recombination”, *J. Chem. Phys.* **71**, 1276 (1979).
- [43] B. Sapoval, “General Formulation of Laplacian Transfer Across Irregular Surfaces”, *Phys. Rev. Lett.* **73**, 3314 (1994).
- [44] D. S. Grebenkov, “Imperfect Diffusion-Controlled Reactions”, in *Chemical Kinetics: Beyond the Textbook*, Eds. K. Lindenberg, R. Metzler, and G. Oshanin (World Scientific, 2019).
- [45] D. S. Grebenkov, “Spectral theory of imperfect diffusion-controlled reactions on heterogeneous catalytic surfaces”, *J. Chem. Phys.* **151**, 104108 (2019).
- [46] S. Redner, *A Guide to First Passage Processes* (Cambridge: Cambridge University press, 2001).
- [47] T. Prüstel and M. Meier-Schellersheim, “Exact Green’s function of the reversible diffusion-influenced reaction for an isolated pair in two dimensions”, *J. Chem. Phys.* **137**, 054104 (2012).
- [48] T. Prüstel and M. Meier-Schellersheim, “Theory of reversible diffusion-influenced reactions with non-Markovian dissociation in two space dimensions”, *J. Chem. Phys.* **138**, 104112 (2013).
- [49] R. Metzler, G. Oshanin, and S. Redner (Eds.) *First-Passage Phenomena and Their Applications* (Singapore: World Scientific, 2014).
- [50] D. Holcman and Z. Schuss, “The Narrow Escape Problem”, *SIAM Rev.* **56**, 213-257 (2014).
- [51] D. C. Torney and H. M. McConnell, “Diffusion-Limited Reaction Rate Theory for Two-Dimensional Systems”, *Proc. Royal Soc. London A* **387**, 147-170 (1983).
- [52] H. S. Carslaw and J. C. Jaeger, *Conduction of Heat in Solids*, 2nd Ed. (Oxford University Press, 1959).
- [53] J. Crank, *The Mathematics of Diffusion*, 2nd Ed. (Oxford University Press, 1975).
- [54] R. K. M. Thambayagam, *The Diffusion Handbook: Applied Solutions for Engineers* (New York: McGraw-Hill Education, 2011).
- [55] M. Smoluchowski, “Versuch einer Mathematischen Theorie der Koagulations Kinetik Kolloider Lösungen”, *Z. Phys. Chem.* **129**, 129-168 (1917).
- [56] M. Galanti, D. Fanelli, S. D. Traytak, and F. Piazza, “Theory of diffusion-influenced reactions in complex geometries”, *Phys. Chem. Chem. Phys.* **18**, 15950 (2016).
- [57] S. D. Traytak and D. S. Grebenkov, “Diffusion-influenced reaction rates for active “sphere-prolate spheroid” pairs and Janus dimers”, *J. Chem. Phys.* **148**, 024107 (2018).
- [58] D. S. Grebenkov and D. Krapf, “Steady-state reaction rate of diffusion-controlled reactions in sheets”, *J. Chem. Phys.* **149**, 064117 (2018).
- [59] D. S. Grebenkov and S. Traytak, “Semi-analytical computation of Laplacian Green functions in three-dimensional domains with disconnected spherical boundaries”, *J. Comput. Phys.* **379**, 91-117 (2019).
- [60] O. Bénichou, C. Chevalier, J. Klafter, B. Meyer, and R. Voituriez, “Geometry-controlled kinetics”, *Nature Chem.* **2**, 472-477 (2010).
- [61] O. Bénichou and R. Voituriez, “From first-passage times of random walks in confinement to geometry-controlled kinetics”, *Phys. Rep.* **539**, 225-284 (2014).
- [62] A. Godec and R. Metzler, “Universal Proximity Effect in Target Search Kinetics in the Few-Encounter Limit”, *Phys. Rev. X* **6**, 041037 (2016).
- [63] D. S. Grebenkov, R. Metzler, and G. Oshanin, “Towards a full quantitative description of single-molecule reaction kinetics in biological cells”, *Phys. Chem. Chem. Phys.* **20**, 16393-16401 (2018).
- [64] D. S. Grebenkov, R. Metzler, and G. Oshanin, “Strong defocusing of molecular reaction times results from an interplay of geometry and reaction control”, *Commun. Chem.* **1**, 96 (2018).
- [65] P. C. Bressloff, B. A. Earnshaw, and M. J. Ward, “Diffusion of protein receptors on a cylindrical dendritic membrane with partially absorbing traps”, *SIAM J. Appl. Math.* **68**, 1223 (2008).

- [66] I. L. Novak, F. Gao, Y.-S. Choi, D. Resasco, J. C. Schaff, and B. M. Slepchenko, “Diffusion on a Curved Surface Coupled to Diffusion in the Volume: Application to Cell Biology”, *J. Comput. Phys.* **226**, 1271-1290 (2007).
- [67] K. Simons and E. Ikonen, “Functional rafts in cell membranes”, *Nature* **387**, 569-572 (1997).
- [68] J.-B. Masson, D. Casanova, S. Türkcan, G. Voisinne, M. R. Popoff, M. Vergassola, and A. Alexandrou, “Inferring maps of forces inside cell membrane microdomains”, *Phys. Rev. Lett.* **102**, 048103 (2009).
- [69] D. Lingwood and K. Simons, “Lipid rafts as a membrane organizing principle”, *Science* **327**, 46-50 (2010).
- [70] D. S. Grebenkov, “First passage times for multiple particles with reversible target-binding kinetics”, *J. Chem. Phys.* **147**, 134112 (2017).
- [71] S. D. Lawley and J. B. Madrid, “First passage time distribution of multiple impatient particles with reversible binding”, *J. Chem. Phys.* **150**, 214113 (2019).
- [72] K. Ritchie, X.-Y. Shan, J. Kondo, K. Iwasawa, T. Fujiwara, and A. Kusumi, “Detection of Non-Brownian Diffusion in the Cell Membrane in Single Molecule Tracking”, *Biophys. J.* **88**, 2266-2277 (2005).
- [73] E. Yamamoto, T. Akimoto, M. Yasui, and K. Yasuoka, Origin of subdiffusion of water molecules on cell membrane surfaces, *Scient. Rep.* **4**, 4720 (2014).
- [74] W. He, H. Song, Y. Su, L. Geng, B. J. Ackerson, H. B. Peng, and P. Tong, Dynamic heterogeneity and non-Gaussian statistics for acetylcholine receptors on live cell membrane, *Nat. Comm.* **7**, 11701 (2016).
- [75] A. V. Chechkin, F. Seno, R. Metzler, and I. M. Sokolov, “Brownian yet Non-Gaussian Diffusion: From Superstatistics to Subordination of Diffusing Diffusivities”, *Phys. Rev. X* **7**, 021002 (2017).
- [76] Y. Lanoiselée, N. Moutal, and D. S. Grebenkov, “Diffusion-limited reactions in dynamic heterogeneous media”, *Nat. Comm.* **9**, 4398 (2018).
- [77] D. S. Grebenkov, “A unifying approach to first-passage time distributions in diffusing diffusivity and switching diffusion models,” *J. Phys. A* **52**, 174001 (2019).
- [78] Y. Lanoiselée and D. S. Grebenkov, “Non-Gaussian diffusion of mixed origins”, *J. Phys. A* **52**, 304001 (2019).
- [79] A. Erdélyi (ed.) *Higher transcendental functions*, Vol. 1 (McGraw-Hill Book Company, New York, 1953).
- [80] E. W. Hobson, *The Theory of Spherical and Ellipsoidal Harmonics* (Cambridge University Press, London, 1931).
- [81] R. N. Hall, “The application of non-integral Legendre functions to potential problems”, *J. Appl. Phys.* **20**, 925-936 (1949).
- [82] W. R. Smythe, *Static and Dynamic Electricity* (McGraw-Hill Book Company, Inc. New York, 1939)
- [83] R. S. Maier, “Legendre functions of fractional degree: transformations and evaluations”, *Proc. R. Soc. A* **472**, 20160097 (2016).
- [84] S. A. Schelkunoff, “Theory of antennas of arbitrary size and shape”, *Proc. I.R.E.* **29**, 493 (1941).
- [85] M. Abramowitz and I. A. Stegun, *Handbook of Mathematical Functions* (Dover Publisher, New York, 1965).
- [86] H. M. MacDonald, “Zeroes of the Spherical Harmonic $P_{nm}(\mu)$ considered as a Function of n ”, *Proc. Lond. Math. Soc.* **31**, 264-281 (1899).
- [87] Digital Library of Mathematical Functions (NIST project), Legendre and Related Functions (<https://dlmf.nist.gov/14.11>)
- [88] R. Szymtkowski, “On the derivative of the Legendre function of the first kind with respect to its degree”, *J. Phys. A* **39**, 15147-15172 (2006).
- [89] H. S. Cohl, “On Parameter Differentiation for Integral Representations of Associated Legendre Functions”, *SIGMA* **7**, 050 (2011).
- [90] R. Courant and D. Hilbert, *Methods of Mathematical Physics* (Wiley-VCH, New York, 1989).
- [91] D. S. Grebenkov and B.-T. Nguyen, “Geometrical structure of Laplacian eigenfunctions”, *SIAM Reviews* **55**, 601-667 (2013).